
LEARNING SYMMETRIC RULES WITH SATNET

Sangho Lim*
School of Computing
KAIST
Daejeon, South Korea
lim.sang@kaist.ac.kr

Eun-Gyeol Oh*
Graduate School of Information Security
KAIST
Daejeon, South Korea
eun-gyeol.oh@kaist.ac.kr

Hongseok Yang
School of Computing and Kim Jaechul Graduate School of AI, KAIST
Discrete Mathematics Group, Institute for Basic Science (IBS)
Daejeon, South Korea
hongseok.yang@kaist.ac.kr

ABSTRACT

SATNet is a differentiable constraint solver with a custom backpropagation algorithm, which can be used as a layer in a deep-learning system. It is a promising proposal for bridging deep learning and logical reasoning. In fact, SATNet has been successfully applied to learn, among others, the rules of a complex logical puzzle, such as Sudoku, just from input and output pairs where inputs are given as images. In this paper, we show how to improve the learning of SATNet by exploiting symmetries in the target rules of a given but unknown logical puzzle or more generally a logical formula. We present SymSATNet, a variant of SATNet that translates the given symmetries of the target rules to a condition on the parameters of SATNet and requires that the parameters should have a particular parametric form that guarantees the condition. The requirement dramatically reduces the number of parameters to learn for the rules with enough symmetries, and makes the parameter learning of SymSATNet much easier than that of SATNet. We also describe a technique for automatically discovering symmetries of the target rules from examples. Our experiments with Sudoku and Rubik's cube show the substantial improvement of SymSATNet over the baseline SATNet.

1 Introduction

Bringing the ability of reasoning to the deep-learning systems has been the aim of a large amount of recent research efforts [Yang et al., 2017, Evans and Grefenstette, 2018, Cingillioglu and Russo, 2019, Wang et al., 2019, Topan et al., 2021]. One notable outcome of these endeavours is SATNet [Wang et al., 2019], a differentiable constraint solver with an efficient custom backpropagation algorithm. SATNet can be used as a component of a deep-learning system and make the system capable of learning and reasoning about sophisticated logical rules. Its potential has been demonstrated successfully with the tasks of learning the rules of complex logical puzzles, such as Sudoku, just from input-output examples where the inputs are given as images.

We show how to improve the rule (or constraint) learning of SATNet, when the target rules have symmetries. By symmetries, we mean transformations of candidate solutions of those rules, and by rules having symmetries, we mean that the solution set of those rules is closed under the transformations of those symmetries. For example, in Sudoku, if a completed 9×9 Sudoku board is a solution, permuting the numbers 1 to 9 in the board, the first three rows, or the last three columns always gives rise to another solution. Thus, these transformations are symmetries of Sudoku.

Our improvement is a variant of SATNet, called SymSATNet, which abbreviates symmetry-aware SATNet. SymSATNet assumes that some symmetries of the target rules are given a priori although the rules themselves are unknown. It then translates these symmetries into a condition on the parameter matrix $C \in \mathbb{R}^{n \times n}$ of SATNet (or our minor

*These authors contributed equally to this work.

generalisation), and requires that the parameters have a particular parametric form that guarantees the condition. Concretely, the translated condition says that the matrix C regarded as a linear map should be equivariant with respect to the group G determined by the given symmetries, and the requirement is that C should be a linear combination of elements in a basis for the space of G -equivariant symmetric matrices. The coefficients of this linear combination are the parameters of our SymSATNet, and their number is often substantially smaller than that of the parameters of SATNet.¹ For Sudoku, the former is 18, while the latter is 729^2 or $k \cdot 729$ for some $k \in \mathbb{N}$ at best. The reduced number of parameters implies that SymSATNet has to tackle an easier learning problem than SATNet, and has a potential to learn faster and generalise better than SATNet.

Who provides symmetries for SymSATNet? The default answer is domain experts, but we show that a better alternative is possible for some applications. We present an algorithm that automatically discovers symmetries. Our algorithm is based on our empirical observation that for Sudoku and a problem related to Rubik’s cube, symmetries emerge in the parameter matrix C of SATNet in the early phase of training, as clusters of similar entries in C . Our algorithm takes a snapshot of the matrix C at some training epoch of SATNet, and searches for a group G such that (i) whenever two entries of C are required to have similar values by the G -equivariance condition, they indeed have such values, and (ii) the number of SymSATNet parameters under G is minimised.

We empirically evaluate SymSATNet and our symmetry-discovering algorithm with Sudoku and a problem related to Rubik’s cube. For both problems, our algorithm discovered nontrivial symmetries, and SymSATNet with manually specified or automatically found symmetries outperformed the baseline SATNet in learning the rules, in terms of both efficiency and generalisation.

Related work There have been multiple studies on discovering symmetries present in conjunctive normal form (CNF) formulas in order to reduce the search space of satisfiability (SAT) solvers. Crawford [1992] proved that the symmetry-detection problem is equivalent to the graph isomorphism problem, and showed how to reduce the complexity of pigeonhole problems using symmetries. Crawford et al. [1996] proposed symmetry-breaking predicates (SBPs), and Aloul et al. [2003, 2006] developed SBPs with more efficient constructions. For automatic symmetry detection, Darga et al. [2004] presented a method that improves the partition refinement procedure introduced by McKay [1976, 1981], and Darga et al. [2008] proposed an algorithm that achieve efficiency by exploiting the sparsity of symmetries. In contrast to these global and static methods, Benhamou et al. [2010], Devriendt et al. [2017] handled local symmetries that dynamically appear during search. In the context of deep learning, Basu et al. [2021], Dehmamy et al. [2021] described algorithms that find and exploit symmetries via group decompositions and Lie algebra convolutions. Our work is also related to the studies on learning logical rules from examples using gradients. Yang et al. [2017] proposed neural logic programming, an end-to-end differentiable system which learns first-order logical rules, Evans and Grefenstette [2018] proposed a differentiable inductive logic programming system which is robust to noise of training data, and Cingillioglu and Russo [2019] introduced an RNN-based model to learn logical reasoning tasks end-to-end. Wang et al. [2018, 2019] presented SATNet using the mixing method, and Topan et al. [2021] further improved SATNet by solving the symbol grounding problem, a key challenge of SATNet. Our work extends these lines of work by proposing how to discover and exploit symmetries when learning logical rules with SATNet.

2 Background

We review SATNet, the formalisation of symmetries using groups, and equivariant maps. For a natural number n , let $[n] = \{1, \dots, n\}$, and for a matrix M , let $M_{i,j}$ be the (i, j) -th entry of M .

2.1 SATNet

A good starting point for learning about SATNet is to look at its origin, the mixing method [Wang et al., 2018], which is an efficient algorithm for solving semidefinite programming problems with diagonal constraints. Let $n, k \in \mathbb{N}$ and C be a real-valued symmetric matrix in $\mathbb{R}^{n \times n}$. The mixing method aims at solving the following optimisation problem:

$$\operatorname{argmin}_{V \in \mathbb{R}^{k \times n}} \langle C, V^T V \rangle \quad \text{subject to } \|v_i\| = 1 \text{ for } i \in [n] \quad (1)$$

where v_i is the i -th column of the matrix V , and $\|v_i\|$ is L_2 norm of v_i . The mixing method solves (1) by coordinate descent, where each column v_i of V is repeatedly updated as follows: $g_i \leftarrow \sum_{j \in [n], j \neq i} C_{i,j} v_j$ and $v_i \leftarrow -\frac{g_i}{\|g_i\|}$. This always finds a fixed point of the equations. In fact, it is shown that almost surely this fixed point attains a global optimum of the optimisation problem.

¹SATNet assumes that C is of the form $S^T S$ for some $S \in \mathbb{R}^{m \times n}$ for $m < n$, so that the number of parameters is $mn < n^2$. But often it is still substantially larger than the number of parameters of SymSATNet.

An example of the above optimisation problem most relevant to us is a continuous relaxation of MAXSAT. MAXSAT is a problem of finding truth assignments to n boolean variables b_1, \dots, b_n . It assumes m clauses of those variables, F_1, \dots, F_m , where F_ℓ is the disjunction of some variables with or without negation: $F_\ell = b_{i_1} \vee \dots \vee b_{i_p} \vee \neg b_{i_{p+1}} \vee \dots \vee \neg b_{i_{p+q}}$. Then, MAXSAT asks for a truth assignment on the variables that maximises the number of true clauses F_i under the assignment. The rules of many problems, including Sudoku, can be expressed as an instance of MAXSAT.

To apply the mixing method to MAXSAT, we introduce relaxed vectors $v_1, \dots, v_n \in \mathbb{R}^k$ that encode the boolean variables, and construct the matrix $S \in \mathbb{R}^{m \times n}$ that encodes the m clauses of MAXSAT: the (ℓ, j) -th entry of S has 1 if F_ℓ contains b_j ; and -1 if F_ℓ includes $\neg b_j$; and 0 if neither of these cases holds. Then, the problem in (1) is formed with $C = -S^T S$, and solved by the mixing method. Our presentation is simplified, and the original version can be found in Wang et al. [2018, 2019].

SATNet is a variant of the mixing method where some of the columns of V are fixed and the optimisation is over the rest of the columns.² Concretely, it assumes that the column indices in $[n]$ are split into two disjoint sets, \mathcal{I} and \mathcal{O} (i.e., $\mathcal{I} \cup \mathcal{O} = [n]$ and $\mathcal{I} \cap \mathcal{O} = \emptyset$). The inputs of SATNet are the columns v_i of V with $i \in \mathcal{I}$, and the outputs are the rest of the columns (i.e., the v_o 's with $o \in \mathcal{O}$). The symmetric matrix C is the parameter of SATNet. Given the input vectors, SATNet repeatedly executes the coordinate descent updates on each output column, until it converges.

One important feature of SATNet is that it has a custom algorithm for backpropagation. Let $V_{\mathcal{I}}$ be the matrix of the input columns to SATNet, and $V_{\mathcal{O}}$ be that of the output columns computed by SATNet on the input $V_{\mathcal{I}}$ under the parameter C . Assume that l is a loss of the output $V_{\mathcal{O}}$. In this context, SATNet provides formulas and algorithms for computing the derivatives $\partial l / \partial V_{\mathcal{I}}$ and $\partial l / \partial C$.

We recall the formulas for the derivatives. Let $o_1 < o_2 < \dots < o_{|\mathcal{O}|}$ be the sorting of the indices in \mathcal{O} . Assume that SATNet was run until convergence, so that the output columns in $V_{\mathcal{O}}$ are the fixed point of the coordinate descent updates: for all $o \in \mathcal{O}$, $g_o = \sum_{j \in [n], j \neq o} C_{o,j} v_j$ and $v_o = -\frac{g_o}{\|g_o\|}$. The formulas for $\partial l / \partial V_{\mathcal{I}}$ and $\partial l / \partial C$ at $(V_{\mathcal{I}}, V_{\mathcal{O}}, C)$ are defined in terms of the next quantities:

$$C', D' \in \mathbb{R}^{|\mathcal{O}| \times |\mathcal{O}|}, \quad P \in \mathbb{R}^{|\mathcal{O}|k \times |\mathcal{O}|k}, \quad U \in \mathbb{R}^{|\mathcal{O}|k \times 1}, \quad W \in \mathbb{R}^{|\mathcal{O}|k \times n^2}.$$

They have the following definitions: for $i, j \in [|\mathcal{O}|]$, $p, q \in [k]$, and $r, s \in [n]$,

$$\begin{aligned} (C')_{i,j} &= \begin{cases} 0 & \text{if } i=j \\ C_{o_i, o_j} & \text{if } i \neq j, \end{cases} & U &= (P((D' + C') \otimes I_k))^\dagger \left(\frac{\partial l}{\partial \text{vec}(V_{\mathcal{O}})} \right)^T, \\ (D')_{i,j} &= \begin{cases} \|g_{o_i}\| & \text{if } i=j \\ 0 & \text{if } i \neq j, \end{cases} & W_{\binom{i-1}{r-1}k+p, \binom{j-1}{s-1}k+q} &= \begin{cases} 0 & \text{if } r = o_i \text{ and } s = o_i \\ V_{p,s} & \text{if } r = o_i \text{ and } s \neq o_i \\ V_{p,s} & \text{if } r \neq o_i \text{ and } s = o_i \\ 0 & \text{if } r \neq o_i \text{ and } s \neq o_i. \end{cases} \\ P_{\binom{i-1}{j-1}k+p, \binom{i-1}{j-1}k+q} &= \begin{cases} (I_k - v_{o_i} v_{o_i}^T)_{p,q} & \text{if } i=j \\ 0 & \text{if } i \neq j, \end{cases} \end{aligned}$$

Here \otimes is the Kronecker product, $_\dagger$ is Moore-Penrose inverse (also known as pseudo inverse), and $\text{vec}(V_{\mathcal{O}})$ is the vector obtained by stacking the columns of $V_{\mathcal{O}}$. Let $C_{\mathcal{O}, \mathcal{I}} \in \mathbb{R}^{|\mathcal{O}| \times |\mathcal{I}|}$ be obtained by restricting C to the indices (o, i) with $o \in \mathcal{O}$ and $i \in \mathcal{I}$. Then,

$$\partial l / \partial \text{vec}(C) = -U^T W, \quad \partial l / \partial \text{vec}(V_{\mathcal{I}}) = -U^T (C_{\mathcal{O}, \mathcal{I}} \otimes I_k). \quad (2)$$

SATNet computes the above derivative formulas efficiently by iterative algorithms.

2.2 Symmetries and equivariant maps

By symmetries on a set \mathcal{X} , we mean a group G that acts on \mathcal{X} . The acting here refers to a function $_ \cdot _$ from $G \times \mathcal{X}$ to \mathcal{X} , called *group action*, such that (i) $e \cdot x = x$ for the unit $e \in G$ and any $x \in \mathcal{X}$, and (ii) $(g \circ g') \cdot x = g \cdot (g' \cdot x)$ for all $g, g' \in G$ and $x \in \mathcal{X}$, where $_ \circ _$ is the group operator of G .

We use symmetries generated from a collection of permutations on a finite set. The set \mathcal{X} in our case is $\mathbb{R}^{k \times n}$, the space of the matrix V in (1), and G is a subgroup of the group \mathcal{S}_n of all permutations on $[n]$. The group action $g \cdot V$ is then defined by permuting the columns of V by g : for all $i, j \in [n]$, $(g \cdot V)_{i,j} = V_{i, g^{-1}(j)}$. This group action can be expressed compactly with the $n \times n$ permutation matrix $P_{g^{-1}}$ where $(P_{g^{-1}})_{i,j} = \mathbf{1}_{\{i=g^{-1}(j)\}}$ and $g \cdot V = V P_{g^{-1}}$ for

²The original SATNet assumes that C has the form $S^T S$ for some $m \times n$ matrix S . We drop this assumption and adjust the forward and backward computations of SATNet accordingly. The main steps of derivations of the formulas for the forward and backward computations are from the work on SATNet [Wang et al., 2019].

the indicator function $\mathbb{1}$. Throughout the paper, we often equate each element g of G with its permutation matrix P_g , and view G itself as the group of permutation matrices P_g for $g \in G$ with the standard matrix multiplication.

One important reason for considering symmetries is to study maps that preserve these symmetries, called equivariant maps. Let G be a group that acts on sets \mathcal{X} and \mathcal{Y} .

Definition 2.1. A function $f : \mathcal{X} \rightarrow \mathcal{Y}$ is *G-equivariant* or *equivariant* if $f(g \cdot x) = g \cdot (f(x))$ for all $g \in G$ and $x \in \mathcal{X}$. It is *G-invariant* or *invariant* if $f(g \cdot x) = f(x)$ for all $g \in G$ and $x \in \mathcal{X}$.

The forms of equivariant maps have been studied extensively in the work on equivariant neural networks and group representation theory [Cohen and Welling, 2016, Maron et al., 2019, Wang et al., 2020]. In particular, when f is linear, various representation theorems for different G 's describe the matrix form of f . We use permutation groups defined inductively by the following three operations.

Definition 2.2. Let G and H be permutation groups on $[p]$ and $[q]$, with each group element viewed as a $p \times p$ or $q \times q$ permutation matrix. The *direct sum* $G \oplus H$, the *direct product* $G \otimes H$, and the *wreath product* $H \wr G$ are the following groups of $(p+q) \times (p+q)$ or $pq \times pq$ permutation matrices with matrix multiplication as their composition:

$$\begin{aligned} G \oplus H &= \{g \oplus h : g \in G, h \in H\}; & G \otimes H &= \{g \otimes h : g \in G, h \in H\}; \\ H \wr G &= \{\text{wr}(\vec{h}, g) : g \in G, \vec{h} \in H^p\}. \end{aligned}$$

Here $g \oplus h$ is the block diagonal matrix with $p \times p$ matrix g as its upper-left corner and $q \times q$ matrix h as the lower-right corner, $g \otimes h$ is the Kronecker product of two matrices g and h , and $\text{wr}(\vec{h}, g)$ is the $pq \times pq$ permutation matrix defined by $\text{wr}(\vec{h}, g)_{(i-1)q+j, (i'-1)q+j'} = \mathbb{1}_{\{g_{i,i'}=(h_i)_{j,j'}=1\}}$ for all $i, i' \in [p]$ and $j, j' \in [q]$.

The next theorem specifies the representation of G -equivariant linear maps for an inductively-constructed G , by describing a basis of the vector space of those linear maps. The theorem can be proved by slightly modifying the argument in Wang et al. [2020]. For a permutation group G on $[m]$, let $\mathcal{E}(G) = \{M \in \mathbb{R}^{m \times m} : gM = Mg, \forall g \in G\}$, the vector space of G -equivariant linear maps, where each $g \in G$ is regarded as a permutation matrix and gM is the multiplication of matrices g and M (i.e., the composition of two linear maps g and M). See Appendix B for the proof of Theorem 2.3.

Theorem 2.3. Let G, H be permutation groups on $[p]$ and $[q]$, and $\mathcal{B}(G), \mathcal{B}(H)$ be some bases of $\mathcal{E}(G)$ and $\mathcal{E}(H)$, respectively. Then, the following sets form bases for $G \oplus H$, $G \otimes H$, and $H \wr G$:

$$\begin{aligned} \mathcal{B}(G \oplus H) &= \{A \oplus \mathbf{0}_q, \mathbf{0}_p \oplus B : A \in \mathcal{B}(G), B \in \mathcal{B}(H)\} \cup \{\mathbf{1}_{O \times (p+O')}, \mathbf{1}_{(p+O') \times O} : O \in \mathcal{O}(G), O' \in \mathcal{O}(H)\}; \\ \mathcal{B}(G \otimes H) &= \{A \otimes B : A \in \mathcal{B}(G), B \in \mathcal{B}(H)\}; \\ \mathcal{B}(H \wr G) &= \{A \otimes \mathbf{1}_{O' \times O''} : A \in \mathcal{B}(G), A_{i,i} = 0 \text{ for } i \in [p], \text{ and } O', O'' \in \mathcal{O}(H)\} \\ &\quad \cup \{I_O \otimes B : B \in \mathcal{B}(H), O \in \mathcal{O}(G)\}. \end{aligned}$$

Here $\mathbf{0}_m$ is an everywhere-zero matrix in $\mathbb{R}^{m \times m}$, and $\mathbf{1}_{R \times S}, I_R$ are the matrices defined by $(\mathbf{1}_{R \times S})_{i,j} = \mathbb{1}_{\{i \in R, j \in S\}}$, $(I_R)_{i,j} = \mathbb{1}_{\{i=j, i \in R\}}$ whose shapes are defined by the context in which they are used. Here, $\mathbf{1}_{O \times (p+O')}, \mathbf{1}_{(p+O') \times O} \in \mathbb{R}^{(p+q) \times (p+q)}$, $\mathbf{1}_{O' \times O''} \in \mathbb{R}^{q \times q}$, $I_O \in \mathbb{R}^{p \times p}$. Also, $\mathcal{O}(G) = \{\{g(i) : g \in G\} : i \in [p]\}$ (i.e., the set of G -orbits), and $p+O = \{p+i : i \in O\}$.

3 Symmetry-aware SATNet

In this section, we present SymSATNet, which abbreviates symmetry-aware SATNet. This variant is designed to operate when symmetries of a learning task are known a priori (via an algorithm or a domain expert). The proofs of the theorem and the lemma in the section are in Appendix C.

SymSATNet solves the optimisation problem of SATNet, but under the following assumptions:

1. The optimisation objective as a map on $\mathbb{R}^{k \times n}$ is invariant with respect to certain symmetries specified by a group G acting on $\mathbb{R}^{k \times n}$, the space of matrices V .
2. The group G and its action are of the type in Section 2.2. That is, each $g \in G$ acts as a permutation on the columns of V . Continuing our convention, we denote P_g by g .

One immediate consequence of these assumptions is that for all $g \in G$ and $V \in \mathbb{R}^{k \times n}$,

$$\langle C, V^T V \rangle = \langle C, (g \cdot V)^T (g \cdot V) \rangle = \langle C, (Vg^{-1})^T (Vg^{-1}) \rangle.$$

The next theorem re-phrases this property of the optimisation objective as equivariance of C :

Theorem 3.1. *Let C be a symmetric $n \times n$ matrix. Then,*

$$\langle C, V^T V \rangle = \langle C, (Vg^{-1})^T (Vg^{-1}) \rangle \quad (3)$$

for all $V \in \mathbb{R}^{k \times n}$ and $g \in G$ if C as a linear map on \mathbb{R}^n is G -equivariant, that is, $Cg = gC$ for all $g \in G$. Furthermore, if $k = n$, the converse also holds.

This theorem lets us incorporate the symmetries into the objective of SATNet, and leaves the handling of the diagonal constraints of SATNet. The next lemma says that those constraints require no special treatment, though, since they are already preserved by the action of any $g \in G$.

Lemma 3.2. *Let $V \in \mathbb{R}^{k \times n}$ and $g \in G$. Every column of V has the L_2 -norm 1 if and only if every column of Vg^{-1} has the L_2 -norm 1.*

Let $\mathcal{E}(G) = \{M \in \mathbb{R}^{n \times n} : Mg = gM, \forall g \in G\}$ be the vector space of G -equivariant matrices and $\mathcal{E}(G)_s$ be the subset of $\mathcal{E}(G)$ containing symmetric matrices. When G is a permutation group constructed inductively by direct sum, direct product, and wreath product, we can generate a basis $\mathcal{B}(G)$ of $\mathcal{E}(G)$ automatically using Theorem 2.3. Then, we can convert $\mathcal{E}(G)$ to an orthogonal basis of $\mathcal{E}(G)_s$ by applying the Gram-Schmidt orthogonalisation to $\{B + B^T : B \in \mathcal{B}(G)\}$. Let $\mathcal{B}(G)_s = \{B_1, \dots, B_d\}$ be such an automatically-generated orthogonal basis of $\mathcal{E}(G)_s$.

SymSATNet is SATNet where the matrix C in the optimisation objective has the form:

$$C = \sum_{\alpha=1}^d \theta_{\alpha} B_{\alpha} \quad (4)$$

for some scalars $\theta_1, \dots, \theta_d \in \mathbb{R}$. Note that by this condition on the form of C , SymSATNet has only d parameters $\theta_1, \dots, \theta_d$, instead of $n \times m$ for some m in the original formulation of SATNet. When the learning target has enough symmetries, d is usually far smaller than n^2 or even n , and this reduction brings speed-up and improved generalisation. Note that (4) amounts to requiring that the optimisation problem of SATNet remain invariant with respect to G ; by Theorem 3.1, it ensures that the optimisation objective is G -invariant, and by Lemma 3.2, the diagonal constraints do not change by the action of any $g \in G$.

The forward computation of SymSATNet is precisely that of SATNet, the repeated coordinate-wise updates until convergence, and the backward computation is the one of SATNet extended (by the chain rule) with a step backpropagating the derivatives $\partial l / \partial C$ to each $\partial l / \partial \theta_{\alpha}$ for $\alpha \in [d]$.³

We summarise SymSATNet below using the usual notation of SATNet (\mathcal{I} , \mathcal{O} , $V_{\mathcal{I}}$, $V_{\mathcal{O}}$, and V):

- The input is $V_{\mathcal{I}}$, the matrix of the input columns of V .
- The parameters are $(\theta_1, \dots, \theta_d) \in \mathbb{R}^d$. They define the matrix C by (4).
- The forward computation solves the following optimisation problem using coordinate descent, and returns $V_{\mathcal{O}}$, the matrix of the output columns of V :

$$\operatorname{argmin}_{V_{\mathcal{O}} \in \mathbb{R}^{k \times |\mathcal{O}|}} \langle C, V^T V \rangle \quad \text{subject to } \|v_o\| = 1 \text{ for } o \in \mathcal{O}.$$

- The backward computation computes $\partial l / \partial V_{\mathcal{I}}$ and $\partial l / \partial \theta_{\alpha}$ by (2) and the chain rule:

$$\partial l / \partial \theta_{\alpha} = (\partial l / \partial \operatorname{vec}(C)) \operatorname{vec}(B_{\alpha}) = -U^T W \operatorname{vec}(B_{\alpha}).$$

4 Discovery of Symmetries

One obstacle for using SymSATNet is that the user has to specify symmetries. We now discuss how to alleviate this issue by presenting an algorithm for discovering candidate symmetries automatically.

The goal of our algorithm, denoted by SYMFIND, is to find a permutation group G that captures the symmetries of an unknown learning target and is expressible by the grammar

$$G ::= \mathcal{I}_m \mid \mathbb{Z}_m \mid \mathcal{S}_m \mid G \oplus G \mid G \otimes G \mid G \wr G,$$

where $m \in \mathbb{N}$. The \mathcal{I}_m denotes the trivial group containing only the identity permutation on $[m]$, and \mathbb{Z}_m denotes the group of cyclic permutations on $[m]$, each of which maps $i \in [m]$ to $(i + n) \bmod m$ for some n . The \mathcal{S}_m is the group of all the permutations on $[m]$. The last three cases are direct sum, direct product, and wreath product (see Definition 2.2).

³SymSATNet is implemented based on the SATNet code [Wang et al., 2019] available under the MIT License.

They describe three ways of decomposing a group G into smaller parts. Having such a decomposition of G brings the benefit that we can recursively and efficiently compute a basis of G -equivariant linear maps.

The design of SYMFIND is based on our empirical observation that a softened version of symmetries often emerges in the parameter matrix C of the original SATNet during training. Even in the early part of training, many entries of C share similar values, and there is a large-enough group G_0 with $Cg \approx gC$ for all $g \in G_0$, which intuitively means that G_0 captures symmetries of C . Furthermore, we observed, G_0 often consists of symmetries of the learning target. This observation suggests an algorithm that takes C as input and finds such a G_0 expressible in our grammar or its slight extension.

The input of SYMFIND is a matrix $M \in \mathbb{R}^{m \times m}$. As previously explained, when SYMFIND is called at the top level, it receives as input the parameter C of SATNet learnt by a fixed number of training steps. However, subsequent recursive calls to SYMFIND may have input M different from C . Then, SYMFIND returns a group G in our grammar and a permutation σ on $[m]$, together defining a permutation group on $[m]$:

$$\text{SYMFIND}(M) = (G, \sigma);$$

$$\text{grp}(G, \sigma) = \{\sigma \circ g \circ \sigma^{-1} : g \in G\},$$

where \circ is the composition of permutations. When G is decomposed into, say $G_1 \oplus G_2$, the σ specifies which indices in $[m]$ get permuted by G_1 and G_2 . Once top-level SYMFIND returns (G, σ) , we construct $\mathcal{B}(\text{grp}(G, \sigma))_s$, as explained in Section 3 with a minor adjustment with σ .⁴

Algorithm 1 describes SYMFIND, where id_m is the identity permutation on $[m]$, $\|\cdot\|_F$ is the Frobenius norm, $\dim(\mathcal{V})$ is the dimension of a vector space \mathcal{V} , and the Reynolds operator prj projects a matrix $M \in \mathbb{R}^{m \times m}$ orthogonally to the subspace of G -equivariant $m \times m$ matrices (i.e., it maps M to the closest G -equivariant matrix in L^2 distance):

$$\text{prj}(G, M) = \frac{1}{|G|} \sum_{g \in G} gMg^T,$$

so that $\|\text{prj}(G, M) - M\|_F$ computes the distance between the matrix M and the space $\mathcal{E}(G)$ of equivariant matrices.

In the lines 2-4, the algorithm first checks whether \mathcal{S}_m models symmetries of the input M accurately. If so, the algorithm returns $(\mathcal{S}_m, \text{id}_m)$. Otherwise, it assumes that an appropriate group for M 's symmetries is one of the remaining cases in the grammar, and constructs a list \mathcal{A} of candidates initially containing the trivial group $(\mathcal{I}_m, \text{id}_m)$. In the lines 6-8, the algorithm adds a pair $(\mathbb{Z}_m, \text{id}_m)$ to \mathcal{A} if the pair approximates M 's symmetries well. In the lines 9-10, it handles the case that M 's symmetries are modelled by a direct sum $\bigoplus_i G'_i$. The algorithm calls the subroutine SUMFIND which returns a group G' of the form $\bigoplus_i G'_i$ and a permutation σ' such that $\text{grp}(G', \sigma')$ approximates M 's symmetries well. The returned group-permutation pair is added to \mathcal{A} . In the lines 11-14, the algorithm calls the other subroutine PRODFIND for every divisor p of m . For each p , PRODFIND finds a group G'' of the form $G''_1 \otimes G''_2$ or $G''_2 \wr G''_1$ and an appropriate permutation σ'' where G''_1 is a permutation group on $[p]$ and G''_2 on $[m/p]$, and $\text{grp}(G'', \sigma'')$ approximates M 's symmetries well. The result of each such call is added to the list \mathcal{A} . Finally, in the line 15, our SYMFIND picks a pair (G, σ) from \mathcal{A} with the strongest level of symmetries in the sense that the basis of $\text{grp}(G, \sigma)$ -equivariant matrices for the selected (G, σ) has the fewest elements.

The subroutine SUMFIND clusters entries of M as blocks since block-shaped clusters commonly arise in matrices equivariant with respect to a direct sum of groups. The other subroutine PRODFIND uses the technique of Van Loan and Pitsianis [1993]; it exploits a typical pattern of Kronecker product of matrices, and detects the presence of the pattern in M by applying SVD to a reshaped version of M . Each subroutine may call SYMFIND recursively. See Appendix D for the details.

5 Experimental Results

We experimentally evaluated SymSATNet and the SYMFIND algorithm on the tasks of learning rules of two problems, namely, Sudoku and what we call completion problem of Rubik's cube. Our evaluation used the original SATNet

⁴We construct $\mathcal{B}(\text{grp}(G, \sigma)) = \{\sigma B \sigma^T : B \in \mathcal{B}(G)\}$, which is an orthogonal basis for $\mathcal{E}(\text{grp}(G, \sigma))$.

Algorithm 1 SYMFIND with a threshold $\lambda > 0$

```

1: Input:  $M \in \mathbb{R}^{m \times m}$       Output:  $(G, \sigma)$ 
2: if  $\|\text{prj}(\text{grp}(\mathcal{S}_m, \text{id}_m), M) - M\|_F \leq \lambda$  then
3:   return  $(\mathcal{S}_m, \text{id}_m)$ 
4: end if
5:  $\mathcal{A} \leftarrow \{(\mathcal{I}_m, \text{id}_m)\}$ 
6: if  $\|\text{prj}(\text{grp}(\mathbb{Z}_m, \text{id}_m), M) - M\|_F \leq \lambda$  then
7:    $\mathcal{A} \leftarrow \mathcal{A} \cup \{(\mathbb{Z}_m, \text{id}_m)\}$ 
8: end if
9:  $(G', \sigma') \leftarrow \text{SUMFIND}(M)$ ;
10:  $\mathcal{A} \leftarrow \mathcal{A} \cup \{(G', \sigma')\}$ 
11: for every divisor  $p$  of  $m$  do
12:    $(G'', \sigma'') \leftarrow \text{PRODFIND}(M, p)$ ;
13:    $\mathcal{A} \leftarrow \mathcal{A} \cup \{(G'', \sigma'')\}$ 
14: end for
15:  $(G, \sigma) \leftarrow \text{argmin}_{(G, \sigma) \in \mathcal{A}} \dim(\mathcal{E}(\text{grp}(G, \sigma)))$ 
16: return  $(G, \sigma)$ 

```

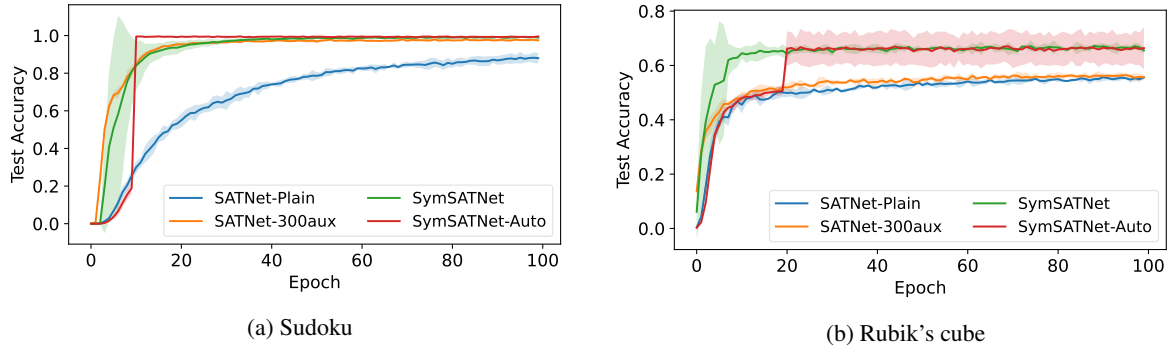


Figure 1: Test accuracies for Sudoku and Rubik’s cube throughout training epochs. We compared our approach with manually-specified symmetries (SymSATNet) and automatically-found symmetries (SymSATNet-Auto) against the baseline SATNet with no auxiliary variables (SATNet-Plain) and with 300 auxiliary variables (SATNet-300aux). Each experiment was repeated 4 times, and its average and 95% confidence interval are reported.

as a baseline, and was under both manually-specified and automatically-discovered symmetries. For SYMFIND, we randomly generated matrices M equivariant with respect to known symmetries and tested whether SYMFIND could recover those symmetries from M . We observed significant improvement of SymSATNet over SATNet in the learning tasks, and also the promising results and limitation of SYMFIND.

Sudoku problem In Sudoku, we are asked to fill in the empty cells of a 9×9 board such that every row, every column, and each of nine 3×3 blocks have all of 1 up to 9. Let $A \in \{0, 1\}^{9 \times 9 \times 9}$ be the encoding of a full number assignment for the board where the (i, j, k) -th entry of A is 1 if the (i, j) -th cell of the board contains k . In SATNet, we flatten A to the assignment on the $n = 9^3 = 729$ boolean variables, and relax each of these variables so that it contains a vector in \mathbb{R}^k , resulting $V \in \mathbb{R}^{k \times n}$ in the optimisation objective of SATNet.

The rules of Sudoku have symmetries formalised by the permutation group $G = (\mathcal{S}_3 \wr \mathcal{S}_3) \otimes (\mathcal{S}_3 \wr \mathcal{S}_3) \otimes \mathcal{S}_9$. Each of two $\mathcal{S}_3 \wr \mathcal{S}_3$ refers to solution-preserving permutations for rows and columns in Sudoku. The last \mathcal{S}_9 refers to permutations of the assigned numbers 1 – 9 in each cell. See Appendix E for more information about the symmetry group for Sudoku.

To learn the rules of Sudoku using SymSATNet, we constructed a basis $\mathcal{B}(G)_s$ as explained in Section 3. It has 18 elements, which means that SymSATNet has 18 parameters to learn.

We used 9K training and 1K test examples generated by the Sudoku generator of Park [2018]. Each example is a pair (V_I, V_O) where the input V_I assigns the values of 39-50 cells (out of 81 cells) and the output V_O specifies the remaining cells. SymSATNet was compared with two types of SATNet: SATNet-Plain without any auxiliary variables, and SATNet-300aux with 300 auxiliary variables. We trained these 3 instances under the binary cross entropy loss and the Adam optimizer [Kingma and Ba, 2015], with the learning rate $\eta = 2 \times 10^{-3}$ for SATNet-Plain and SATNet-300aux as in the original work on SATNet, and $\eta = 4 \times 10^{-2}$ for SymSATNet. We measured test accuracy, which is the average number of the correctly-solved Sudoku instances in the 1K test set by the forward computations of SymSATNet, SATNet-Plain, and SATNet-300aux. Each of our experiments was run four times, and we report the average with 95% confidence interval in each run.

MODEL	SUDOKU		CUBE	
	ACC.	TIME	ACC.	TIME
SATNET-PLAIN	88.3%	48.4	55.7%	1.8
	$\pm 3.1\%$	± 0.3	$\pm 1.4\%$	± 0.01
SATNET-300AUX	98.0%	91.0	56.5%	14.3
	$\pm 0.4\%$	± 1.1	$\pm 0.6\%$	± 0.19
SYMSATNET	99.3%	25.7	67.2%	1.1
	$\pm 0.5\%$	± 0.2	$\pm 0.6\%$	± 0.00
SYMSATNET-AUTO	99.6%	23.1	67.1%	2.6
	$\pm 0.2\%$	± 0.6	$\pm 6.3\%$	± 1.37

Table 1: Best test accuracies during 100 epochs and average train times (sec/epoch) for Sudoku and Rubik’s cube. The reported numbers are averaged over four runs, and the 95% confidence intervals are also included.

The results are in Figure 1 and Table 1. (SymSATNet-Auto is SymSATNet with our automatic symmetry-discovery algorithm, and will be described in a later part of this section.) Our SymSATNet outperformed SATNet-Plain and SATNet-300aux. On average, its training run for 100 iterations finished 2-4 \times faster in terms of wall clock than those of these two alternatives. This is due to the reduced number of parameters and avoidance of certain matrix operations. See Appendix F for more information about the operations in SymSATNet. Despite the speed up, the best

test accuracy of SymSATNet (99.3%) on average was significantly better than SATNet-Plain (88.3%) and slightly better than SATNet-300aux (98.0%).

Completion problem of Rubik’s cube The standard Rubik’s cube is composed of 6 faces, each of which has 9 facelets. We considered a constraint satisfaction problem related to Rubik’s cube where we are given a partial colour assignment of facelets, and then asked to complete the remaining facelets such that the resulting colour assignment is solvable; by moving the cube, we can make all facelets in each face have the same colour, and no same colours appear in two faces.

Let $A \in \{0, 1\}^{6 \times 9 \times 6}$ be a colour assignment of Rubik’s cube where the (i, j, k) -th entry has 1 if and only if the j -th facelet of the i -th face has colour k . We formulate the optimisation objective of SATNet for Rubik’s cube using the relaxation of such an assignment A to $V \in \mathbb{R}^{k \times n}$ for $n = 6 \times 9 \times 6$.

This problem has symmetries formalised by a group $G = \mathcal{R}_{54} \otimes \mathcal{R}_6$ on $[n]$. Here \mathcal{R}_{54} and \mathcal{R}_6 are permutation groups on [54] and [6], each of which captures the allowed rotations of facelets, and the rotations of the whole cube. If a colour assignment A is solvable, so is the transformation of A by any permutations in G . See Appendix E for more information about the symmetries of this problem.

We generated a basis $\mathcal{B}(G)_s$ in three steps. We first created $\mathcal{B}(\mathcal{R}_{54})$ and $\mathcal{B}(\mathcal{R}_6)$ using the technique of Finzi et al. [2021]. Next, we combined them using Theorem 2.3, and got $\mathcal{B}(G)$, which was converted to a symmetric orthogonal basis $\mathcal{B}(G)_s$ via Gram-Schmidt. The final result has 48 basis elements.

We used a dataset of 9K training and 1K test examples generated by randomly applying moves to the solution of the cube. Each example is a pair (V_I, V_O) where V_I assigns colours to facelets except for two corner facelets, two edge facelets, and one center facelet, and V_O specifies the colours of those five missing facelets. In the test examples, only V_I is used. We trained SymSATNet, SATNet-Plain, and SATNet-300aux for 100 epochs, under the same configuration as in the Sudoku case.

The results appear in Figure 1 and Table 1. (SymSATNet-Auto will be described below.) On average, the 100-epoch training of SymSATNet completed faster in the wall-clock time than those of SATNet-Plain and SATNet-300aux. Also, it achieved better test accuracies (67.2%) than these alternatives (55.7% and 56.5%). Note that unlike Sudoku, the test accuracy of SATNet-300aux was only marginally better than that of SATNet-Plain, which indicates that both suffered from the overfitting issue. Note also the sharp increase in the training time of SATNet-300aux. These two indicate that adding auxiliary variables is not so effective for the completion problem for Rubik’s cube, while exploiting symmetries is still useful as indicated by the performance of SymSATNet.

Automatic discovery of symmetries To test the effectiveness of SYMFIND, we tested whether SYMFIND could find proper symmetries in Sudoku and Rubik’s cube. We trained SATNet-Plain for 10-epochs in Sudoku and 20-epochs in Rubik’s cube, and applied SYMFIND to the parameter matrices C . For Sudoku, SYMFIND always recovered the full symmetries with $G = (\mathcal{S}_3 \wr \mathcal{S}_3) \otimes (\mathcal{S}_3 \wr \mathcal{S}_3) \otimes \mathcal{S}_9$ in our 10 trials. For Rubik’s cube, the group of full symmetries is $\text{grp}(G, \sigma)$ for $G = ((\mathcal{S}_2 \wr \mathcal{S}_3) \oplus (\mathcal{S}_3 \wr \mathcal{S}_8) \oplus (\mathcal{S}_2 \wr \mathcal{S}_{12})) \otimes (\mathcal{S}_2 \wr \mathcal{S}_3)$. SYMFIND recovered all the parts except $\mathcal{S}_2 \wr \mathcal{S}_{12}$. Instead of this, the algorithm found $\mathcal{S}_{12} \otimes \mathcal{S}_2$ or $\mathcal{S}_3 \otimes \mathcal{S}_8$, or $\mathcal{S}_4 \otimes \mathcal{S}_6$ in our 10 trials. We manually observed that the entries of C in the portion of $\mathcal{S}_2 \wr \mathcal{S}_{12}$ part were difficult to be clustered, violating the assumption of SYMFIND. This illustrates the fundamental limitation of SYMFIND.

To account for the limitation of SYMFIND, we refined the group G of detected symmetries to a subgroup in an additional validation step, before training SymSATNet with those symmetries. In the validation step, we checked the usefulness of each part G_i of the expression of G in our grammar. Concretely, we rewrote G only with the part G_i in concern, where all the other parts of G were masked by the trivial groups \mathcal{I}_k . Let G'_i be the resulting group of this rewriting. Then, we projected C onto the space of G'_i -equivariant matrices using the corresponding Reynolds operator, and measured the accuracy of SATNet with C before and after the projection over validation examples. Finally, we kept the parts G_i that led to the improvement of validation accuracy larger than a threshold, and assembled such parts to get G' , which was finally used to train SymSATNet. For example, if $G = (\mathbb{Z}_3 \otimes \mathcal{S}_4) \oplus \mathcal{S}_5$ is discovered by SYMFIND, we consider the parts $G_1 = \mathbb{Z}_3$, $G_2 = \mathcal{S}_4$, and $G_3 = \mathcal{S}_5$. Then, we construct three groups $G'_1 = (\mathbb{Z}_3 \otimes \mathcal{I}_4) \oplus \mathcal{I}_5$, $G'_2 = (\mathbb{Z}_3 \otimes \mathcal{S}_4) \oplus \mathcal{I}_5$, and $G'_3 = (\mathbb{Z}_3 \otimes \mathcal{I}_4) \oplus \mathcal{S}_5$, and measure the accuracy of SATNet with C projected by each G'_i over validation examples. If G'_1 and G'_3 show accuracy improvements greater than a threshold, we combine G_1 and G_3 to form $G' = (\mathbb{Z}_3 \otimes \mathcal{I}_4) \oplus \mathcal{S}_5$, which is then used to train SymSATNet.

We used 8K training, 1K validation, and 1K test examples to train SymSATNet with symmetries found by SYMFIND and the validation step. We denote these runs by SymSATNet-Auto. For Sudoku, we took a group G discovered from the SATNet-Plain parameter C at the 10-th training epoch, constructed its subgroup G' via the validation step, and computed an orthogonal basis $\mathcal{B}(G')_s$. SymSATNet was then trained after being initialised by the projection of C

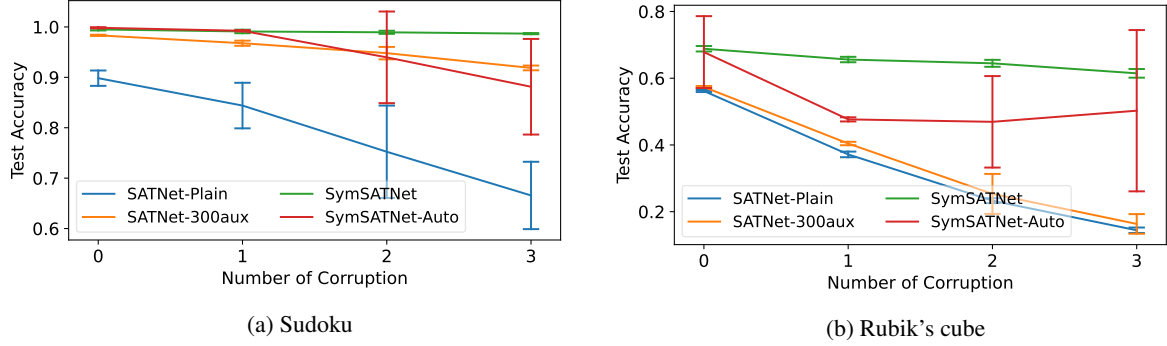


Figure 2: Best test accuracies for noisy Sudoku and Rubik's cube datasets. We compared our approaches (SymSATNet, SymSATNet-Auto) against the baselines (SATNet-Plain, SATNet-300aux) by training them with noise-corrupted datasets. Each experiment was repeated 3 times, and its average and 95% confidence interval are reported.

with $\mathcal{B}(G')_s$. The same process was applied to Rubik's cube, but with C taken at the 20-th training epoch. The other configurations are the same as in our experiments with manually-specified symmetries.

As shown in Figure 1 and Table 1, SymSATNet-Auto performed the best for Sudoku (99.6%), better than even SymSATNet. For Rubik's cube, SymSATNet-Auto (67.1%) also outperformed SATNet-Plain and SATNet-300aux. During the four trials with Sudoku, SymSATNet-Auto was always given the full symmetries in Sudoku. In two of the four trials with Rubik's cube, SymSATNet-Auto was given correct subgroups $((\mathcal{S}_2 \wr \mathcal{S}_3) \oplus (\mathcal{S}_3 \wr \mathcal{S}_8) \oplus (\mathcal{I}_4 \otimes \mathcal{I}_6)) \otimes (\mathcal{S}_2 \wr \mathcal{S}_3)$ and $((\mathcal{S}_2 \wr \mathcal{S}_3) \oplus (\mathcal{S}_3 \wr (\mathcal{S}_2 \wr \mathcal{S}_4)) \oplus (\mathcal{I}_8 \otimes \mathcal{I}_3)) \otimes (\mathcal{S}_2 \wr \mathcal{S}_3)$, and performed even better than SymSATNet. In the other trials, SymSATNet-Auto exploited slightly incorrect symmetries, but it outperformed SATNet-Plain and SATNet-300aux. These results show that exploiting the partial symmetries of subgroups derived by the validation step are still useful for learning, even when the symmetries are slightly inaccurate.

Robustness to noise We tested robustness of SymSATNet and SymSATNet-Auto to noise by training them with noise-corrupted datasets. We generated noisy Sudoku and Rubik's cube datasets where each training example has a randomly-chosen cell or facelet corrupted with noise: the noise alters the value of the cell or the colour of the facelet to a random value other than the original. We used noisy datasets with 0-3 corrupted instances to measure the test accuracy, and tried three runs for each dataset to report the average and 95% confidence interval. All the other setups are the same as before. Figure 2 shows the results. In both problems, SymSATNet was the most robust to noise, showing remarkably consistent accuracies. SymSATNet-Auto showed comparable robustness to SATNet-300aux in noisy Sudoku, but outperformed the two baselines in noisy Rubik's cube.

Next, to show the robustness of SYMFIND, we applied the algorithm to the problem of restoring a permutation group G from a noise-corrupted G -equivariant symmetric matrix M . We picked four group-permutation pairs (G_i, σ_i) for $i \in [4]$ where $\sigma_1, \sigma_2, \sigma_3$ are random permutations on [15], [30], [12], and σ_4 is the identity permutation on [8], and

$$G_1 = \mathbb{Z}_3 \oplus \mathbb{Z}_3 \oplus \mathbb{Z}_3 \oplus \mathbb{Z}_3 \oplus \mathbb{Z}_3, \quad G_2 = \mathcal{S}_3 \wr \mathcal{S}_{10}, \quad G_3 = (\mathcal{S}_3 \wr \mathcal{S}_3) \oplus \mathbb{Z}_3, \quad G_4 = \mathcal{S}_2 \otimes \mathcal{S}_2 \otimes \mathcal{S}_2.$$

Then, we generated $\text{grp}(G_i, \sigma_i)$ -equivariant symmetric matrices M_i by projecting random matrices with standard normal entries into the space $\mathcal{E}(\text{grp}(G_i, \sigma_i))_s$. Then, Gaussian noises from $\mathcal{N}(0, \omega^2)$ for $\omega = 5 \times 10^{-3}$ are added to M_i 's entries, and the resulting matrix M'_i is given to SYMFIND.

For each (G_i, σ_i) , we repeatedly generated M'_i and ran SYMFIND on M'_i for 1K times, and measured the portion of cases out of 1K where SYMFIND recovered (G_i, σ_i) exactly (full accuracy), and also the portion of cases where SYMFIND returned a subgroup of (G_i, σ_i) which is not the trivial group \mathcal{I}_m (partial accuracy). As Table 2 shows, the measured full accuracies were in the range of 60.3 – 93.5%, and the partial accuracies were in the range of 79.2 – 94.3%. These results show the ability of SYMFIND to recover meaningful and sometimes full symmetries.

GROUP	FULL ACC.	PARTIAL ACC.
$\bigoplus_{i=1}^5 \mathbb{Z}_3$	76.6%	79.2%
$\mathcal{S}_3 \wr \mathcal{S}_{10}$	60.3%	79.9%
$(\mathcal{S}_3 \wr \mathcal{S}_3) \oplus \mathbb{Z}_3$	77.5%	87.0%
$\mathcal{S}_2 \otimes \mathcal{S}_2 \otimes \mathcal{S}_2$	93.5%	94.3%

Table 2: Full accuracies and partial accuracies of SYMFIND for group symmetries over 1K runs.

6 Conclusion

We presented SymSATNet, a symmetry-aware variant of SATNet, that is capable of exploiting symmetries of the rules or constraints to be learnt by SymSATNet. We also described an algorithm for automatically discovering symmetries from the parameter C of the original SATNet at a fixed training epoch, which is based on our empirical observation that symmetries emerge during training as duplicated or similar entries of C . Our experimental evaluations with two rule-learning problems related to Sudoku and Rubik’s cube show the benefit of SymSATNet and the promise and limitation of our symmetry-discovering algorithm. Interesting future research directions are to analyse symmetry emergence in SATNet mathematically and to analyse the formal properties of our symmetry-discovering algorithm, such as when it can recover full symmetries.

Acknowledgements

This work was supported by the Engineering Research Center Program through the National Research Foundation of Korea (NRF) funded by the Korean Government MSIT (NRF-2018R1A5A1059921) and also by the Institute for Basic Science (IBS-R029-C1).

References

- Fadi A Aloul, Arathi Ramani, Igor L Markov, and Karem A Sakallah. Solving difficult instances of boolean satisfiability in the presence of symmetry. *IEEE Transactions on Computer-Aided Design of Integrated Circuits and Systems*, 22(9):1117–1137, 2003.
- Fadi A Aloul, Karem A Sakallah, and Igor L Markov. Efficient symmetry breaking for boolean satisfiability. *IEEE Transactions on Computers*, 55(5):549–558, 2006.
- Sourya Basu, Akshayaa Magesh, Harshit Yadav, and Lav R Varshney. Group equivariant neural architecture search via group decomposition and reinforcement learning. *arXiv e-prints*, pages arXiv–2104, 2021.
- Belaid Benhamou, Tarek Nabhani, Richard Ostrowski, and Mohamed Réda Sardi. Dynamic symmetry breaking in the satisfiability problem. In *Proceedings of the 16th international conference on Logic for Programming, Artificial intelligence, and Reasoning. LPAR-16, Dakar, Senegal (April 25-may 1, 2010)*, 2010.
- Nuri Cingillioglu and Alessandra Russo. Deeplogic: Towards end-to-end differentiable logical reasoning. In *Proceedings of the AAAI 2019 Spring Symposium on Combining Machine Learning with Knowledge Engineering (AAAI-MAKE 2019)*, 2019.
- Taco S. Cohen and Max Welling. Group equivariant convolutional networks. In *Proceedings of ICML’16*, pages 2990–2999, 2016.
- James Crawford. A theoretical analysis of reasoning by symmetry in first-order logic. In *AAAI Workshop on Tractable Reasoning*, pages 17–22. Citeseer, 1992.
- James M. Crawford, Matthew L. Ginsberg, Eugene M. Luks, and Amitabha Roy. Symmetry-breaking predicates for search problems. In *Proceedings of the Fifth International Conference on Principles of Knowledge Representation and Reasoning*, pages 148–159. Morgan Kaufmann Publishers Inc., 1996.
- Paul T. Darga, Mark H. Liffiton, Karem A. Sakallah, and Igor L. Markov. Exploiting structure in symmetry detection for cnf. In *Proceedings of the 41st Annual Design Automation Conference*, pages 530–534. Association for Computing Machinery, 2004.
- Paul T Darga, Karem A Sakallah, and Igor L Markov. Faster symmetry discovery using sparsity of symmetries. In *2008 45th ACM/IEEE Design Automation Conference*, pages 149–154. IEEE, 2008.
- Nima Dehmamy, Robin Walters, Yan Chen Liu, Dashun Wang, and Rose Yu. Automatic symmetry discovery with lie algebra convolutional network. *Advances in Neural Information Processing Systems*, 34, 2021.
- Jo Devriendt, Bart Bogaerts, and Maurice Bruynooghe. Symmetric explanation learning: Effective dynamic symmetry handling for sat. In *International Conference on Theory and Applications of Satisfiability Testing*, pages 83–100. Springer, 2017.
- David S Dummit and Richard M Foote. *Abstract algebra*, volume 1999. Prentice Hall Englewood Cliffs, NJ, 1991.
- Richard Evans and Edward Grefenstette. Learning explanatory rules from noisy data. *J. Artif. Intell. Res.*, 61:1–64, 2018.
- Marc Finzi, Max Welling, and Andrew Gordon Wilson. A practical method for constructing equivariant multilayer perceptrons for arbitrary matrix groups. In *Proceedings of ICML’21*, pages 3318–3328, 2021.

- Diederik P. Kingma and Jimmy Ba. Adam: A method for stochastic optimization. *CoRR*, abs/1412.6980, 2015.
- Subrata Majumdar, Kalyan Kumar Dey, and Mohd Altab Hossain. Direct product and wreath product of transformation semigroups. *GANIT: Journal of Bangladesh Mathematical Society*, 31:1–7, Apr. 2012.
- Haggai Maron, Heli Ben-Hamu, Nadav Shamir, and Yaron Lipman. Invariant and equivariant graph networks. In *Proceedings of ICLR'19*, 2019.
- Brendan D. McKay. *Backtrack programming and the graph isomorphism problem*. PhD thesis, University of Melbourne, 1976.
- Brendan D. McKay. Practical graph isomorphism. *Congressus Numerantium*, 30:45–87, 1981.
- Kyubyong Park. Can convolutional neural networks crack sudoku puzzles? <https://github.com/Kyubyong/sudoku>, 2018.
- Sever Topan, David Rolnick, and Xujie Si. Techniques for symbol grounding with satnet. In *Advances in Neural Information Processing Systems*, volume 34, pages 20733–20744. Curran Associates, Inc., 2021.
- Charles F Van Loan and Nikos Pitsianis. Approximation with kronecker products. In *Linear algebra for large scale and real-time applications*, pages 293–314. Springer, 1993.
- Po-Wei Wang, Wei-Cheng Chang, and J. Zico Kolter. The mixing method: low-rank coordinate descent for semidefinite programming with diagonal constraints. *CoRR*, abs/1706.00476, 2018.
- Po-Wei Wang, Priya L. Donti, Bryan Wilder, and J. Zico Kolter. Satnet: Bridging deep learning and logical reasoning using a differentiable satisfiability solver. In *Proceedings of ICML'19*, pages 6545–6554, 2019. URL <https://github.com/locuslab/SATNet.git>.
- Renhao Wang, Marjan Albooyeh, and Siamak Ravanbakhsh. Equivariant networks for hierarchical structures. In *Proceedings of NeurIPS'20*, pages 13806–13817, 2020.
- Fan Yang, Zhilin Yang, and William W. Cohen. Differentiable learning of logical rules for knowledge base reasoning. In *Proceedings of NeurIPS'17*, pages 2319–2328, 2017.

A Notation

For natural numbers n_1 and n_2 with $n_1 \leq n_2$, we write $[n_1 : n_2]$ for the set $\{n_1, n_1 + 1, \dots, n_2\}$. For an $m \times m$ matrix M , $1 \leq a \leq b \leq m$, and $1 \leq c \leq d \leq m$, we define $M[a : b, c : d]$ by a $(b - a + 1) \times (d - c + 1)$ matrix M :

$$M[a : b, c : d]_{i,j} = M_{a+i-1, c+j-1} \quad \text{for } i \in [b - a + 1] \text{ and } j \in [d - c + 1].$$

Also, if H is a subgroup of G , we denote it by $H \leq G$.

B Proof of Theorem 2.3

In this section, we prove Theorem 2.3. Here we prove the direct sum, direct product, and wreath product cases by an argument similar to the one in Wang et al. [2020]. For the wreath product case, we slightly generalise the results in Wang et al. [2020], which considered only transitive group actions. We will use the notation from Theorem 2.3. Let G and H be permutation groups over $[p]$ and $[q]$, respectively. Also, let $A \in \mathcal{B}(G)$, $B \in \mathcal{B}(H)$, $O \in \mathcal{O}(G)$, and $O', O'' \in \mathcal{O}(H)$.

Claim B.1. *The matrices $A \oplus \mathbf{0}_q$, $\mathbf{0}_p \oplus B$, $\mathbf{1}_{O \times (p+O')}$, and $\mathbf{1}_{(p+O) \times O'}$ are $(G \oplus H)$ -equivariant. Also, the matrices of these types for all possible choices of A , B , O , and O' form a linearly independent set.*

Proof. Pick arbitrary group elements $g \in G$ and $h \in H$. Let P_g and P_h be the permutation matrices corresponding to g and h , respectively.

We prove the claimed equivariance below:

$$\begin{aligned} (P_g \oplus P_h)(A \oplus \mathbf{0}_p) &= (P_g A) \oplus \mathbf{0}_p = (AP_g) \oplus \mathbf{0}_p = (A \oplus \mathbf{0}_p)(P_g \oplus P_h), \\ (P_g \oplus P_h)(\mathbf{0}_q \oplus B) &= \mathbf{0}_q \oplus (P_h B) = \mathbf{0}_q \oplus (BP_h) = (\mathbf{0}_q \oplus B)(P_g \oplus P_h), \\ (P_g \oplus P_h)\mathbf{1}_{O \times (p+O')} &= \mathbf{1}_{O \times (p+O')} = \mathbf{1}_{O \times (p+O')}(P_g \oplus P_h), \\ (P_g \oplus P_h)\mathbf{1}_{(p+O') \times O} &= \mathbf{1}_{(p+O') \times O} = \mathbf{1}_{(p+O') \times O}(P_g \oplus P_h). \end{aligned}$$

The third and fourth lines use the fact that $\mathbf{1}_{O \times (p+O')}$ and $\mathbf{1}_{(p+O') \times O}$ are invariant under the left or right multiplication of the permutation matrix $P_g \oplus P_h$. This holds because the orbits of G are preserved by any permutation in G , and those of H are preserved by all permutations in H , so that

$$\begin{aligned} P_g \mathbf{1}_{O \times O'} &= \mathbf{1}_{O \times O'} = \mathbf{1}_{O \times O'} P_h, \\ P_h \mathbf{1}_{O' \times O} &= \mathbf{1}_{O' \times O} = \mathbf{1}_{O' \times O} P_g. \end{aligned} \tag{5}$$

Next, we show the claimed linear independence by analysing the indices of the nonzero entries of the four types of matrices in the claim.

1. The matrices of the type $A \oplus \mathbf{0}_q$ for some $A \in \mathcal{B}(G)$ are linearly independent, since their A parts are linearly independent.
2. The matrices of the type $\mathbf{0}_p \oplus B$ for some $B \in \mathcal{B}(H)$ are also linearly independent by similar reason.
3. Different matrices of the type $\mathbf{1}_{O \times (p+O')}$ for some O and O' do not share an index of a nonzero entry, since different orbits of a group are disjoint. Thus, the matrices of this type are linearly independent.
4. Different matrices of the type $\mathbf{1}_{(p+O) \times O'}$ for some O and O' do not share an index of a nonzero entry. Thus, the matrices of this form are linearly independent.

Also, any matrices of the above four types form a linearly independent set because those linear combinations do not share any indices of nonzero entries. From this and the above reasoning for each of the four types of matrices it follows that the matrices of those four types are linearly independent, as claimed. \square

Claim B.2. *The matrix $A \otimes B$ is $(G \otimes H)$ -equivariant. Also, the matrices of this shape for all possible choices of A and B form a linearly independent set.*

Proof. Pick arbitrary group elements $g \in G$ and $h \in H$. Let P_g and P_h be the permutation matrices corresponding to g and h , respectively. Then,

$$(P_g \otimes P_h)(A \otimes B) = (P_g A) \otimes (P_h B) = (AP_g) \otimes (BP_h) = (A \otimes B)(P_g \otimes P_h).$$

For linear independence, we can prove it using the fact $\langle A \otimes B, A' \otimes B' \rangle = \langle A, A' \rangle \cdot \langle B, B' \rangle$. \square

Claim B.3. *The matrices $A \otimes \mathbf{1}_{O' \times O''}$ such that $A_{i,i} = 0$ for $i \in [p]$ and $I_O \otimes B$ are $(H \wr G)$ -equivariant. Also, the matrices of these types for all possible choices of $A, B, O, O',$ and O'' form a linearly independent set.*

Proof. Pick arbitrary group elements $g \in G$ and $\vec{h} = (h_1, \dots, h_p) \in H^p$. Let $P_{g^{-1}}$ and P_{h_i} be the permutation matrices corresponding to g^{-1} and h_i for $i \in [p]$. We can express $\text{wr}(\vec{h}, g)$ and $P_{g^{-1}}$ by

$$\text{wr}(\vec{h}, g) = \sum_{i=1}^p \mathbf{1}_{\{i\} \times \{g(i)\}} \otimes P_{h_i}, \quad P_{g^{-1}} = \sum_{i=1}^p \mathbf{1}_{\{i\} \times \{g(i)\}}.$$

Then, we prove the following equivariance:

$$\begin{aligned} \text{wr}(\vec{h}, g) (A \otimes \mathbf{1}_{O' \times O''}) &= \left(\sum_{i=1}^p \mathbf{1}_{\{i\} \times \{g(i)\}} \otimes P_{h_i} \right) (A \otimes \mathbf{1}_{O' \times O''}) \\ &= \sum_{i=1}^p (\mathbf{1}_{\{i\} \times \{g(i)\}} A \otimes P_{h_i} \mathbf{1}_{O' \times O''}) \\ &= \left(\sum_{i=1}^p \mathbf{1}_{\{i\} \times \{g(i)\}} \right) A \otimes \mathbf{1}_{O' \times O''} \end{aligned} \tag{6}$$

$$\begin{aligned} &= P_{g^{-1}} A \otimes \mathbf{1}_{O' \times O''} = A P_{g^{-1}} \otimes \mathbf{1}_{O' \times O''} \\ &= A \left(\sum_{i=1}^p \mathbf{1}_{\{i\} \times \{g(i)\}} \right) \otimes \mathbf{1}_{O' \times O''} \\ &= \sum_{i=1}^p (A \mathbf{1}_{\{i\} \times \{g(i)\}} \otimes \mathbf{1}_{O' \times O''} P_{h_i}) \end{aligned} \tag{7}$$

$$\begin{aligned} &= (A \otimes \mathbf{1}_{O' \times O''}) \left(\sum_{i=1}^p \mathbf{1}_{\{i\} \times \{g(i)\}} \otimes P_{h_i} \right) \\ &= (A \otimes \mathbf{1}_{O' \times O''}) \text{wr}(\vec{h}, g), \end{aligned}$$

$$\begin{aligned} \text{wr}(\vec{h}, g) (I_O \otimes B) &= \left(\sum_{i=1}^p \mathbf{1}_{\{i\} \times \{g(i)\}} \otimes P_{h_i} \right) (I_O \otimes B) \\ &= \sum_{i=1}^p (\mathbf{1}_{\{i\} \times \{g(i)\}} I_O \otimes P_{h_i} B) \\ &= \sum_{i=1}^p (\mathbf{1}_{\{i\} \times (\{g(i)\} \cap O)} \otimes P_{h_i} B) \\ &= \sum_{i=1}^p (\mathbf{1}_{(\{i\} \cap O) \times \{g(i)\}} \otimes B P_{h_i}) \\ &= \sum_{i=1}^p (I_O \mathbf{1}_{\{i\} \times \{g(i)\}} \otimes B P_{h_i}) \\ &= (I_O \otimes B) \left(\sum_{i=1}^p \mathbf{1}_{\{i\} \times \{g(i)\}} \otimes P_{h_i} \right) \\ &= (I_O \otimes B) \text{wr}(\vec{h}, g). \end{aligned} \tag{8}$$

Here, (6) and (7) use the same argument in (5), and (8) uses the fact that $i \in O \iff g(i) \in O$ for any $g \in G$ and $O \in \mathcal{O}(G)$. For linear independence, we again use the fact $\langle A \otimes B, A' \otimes B' \rangle = \langle A, A' \rangle \cdot \langle B, B' \rangle$ to show the orthogonality of all possible matrices of types $A \otimes \mathbf{1}_{O' \times O''}$ and $I_O \otimes B$. \square

Claim B.4. *The number of basis elements of $G \oplus H$, $G \otimes H$, and $H \wr G$ can be computed as follows:*

$$\begin{aligned} |\mathcal{B}(G \oplus H)| &= |\mathcal{B}(G)| + |\mathcal{B}(H)| + 2|\mathcal{O}(G)||\mathcal{O}(H)|, \\ |\mathcal{B}(G \otimes H)| &= |\mathcal{B}(G)||\mathcal{B}(H)|, \\ |\mathcal{B}(H \wr G)| &= |\mathcal{O}(G)||\mathcal{B}(H)| + (|\mathcal{B}(G)| - |\mathcal{O}(G)|)|\mathcal{O}(H)|^2. \end{aligned}$$

Proof. First, we derive some general fact on a finite permutation group. Let \mathbf{G} be a permutation group on $[r]$ for some r . Consider the action of \mathbf{G} on the space of r -dimensional vectors $\mathcal{X} = \mathbb{R}^r$ by the row permutation action $g \cdot v = P_g v$ for any $g \in \mathbf{G}$. Define $\mathcal{F}(\mathbf{G}) = \{v \in \mathcal{X} : g \cdot v = v, \forall g \in \mathbf{G}\}$. Consider the following linear operator

$$\phi_{\mathbf{G}} : \mathcal{X} \rightarrow \mathcal{X}, \quad \phi_{\mathbf{G}}(v) = \frac{1}{|\mathbf{G}|} \sum_{g \in \mathbf{G}} g \cdot v,$$

which can also be represented as the following matrix:

$$\phi_{\mathbf{G}} = \frac{1}{|\mathbf{G}|} \sum_{g \in \mathbf{G}} P_g.$$

Since

$$\begin{aligned} \phi_{\mathbf{G}}(\phi_{\mathbf{G}}(v)) &= \frac{1}{|\mathbf{G}|^2} \sum_{g_1 \in \mathbf{G}} \sum_{g_2 \in \mathbf{G}} g_1 \cdot (g_2 \cdot v) \\ &= \frac{1}{|\mathbf{G}|^2} \sum_{g_1 \in \mathbf{G}} \sum_{g_2 \in \mathbf{G}} (g_1 \circ g_2) \cdot v \\ &= \frac{1}{|\mathbf{G}|^2} \sum_{g_1 \in \mathbf{G}} \sum_{g \in \mathbf{G}} g \cdot v \\ &= \frac{1}{|\mathbf{G}|} \sum_{g \in \mathbf{G}} g \cdot v, \end{aligned}$$

the operator $\phi_{\mathbf{G}}$ is a projection map. Also, we have $\text{im}(\phi_{\mathbf{G}}) = \mathcal{F}(\mathbf{G})$ where $\text{im}(f)$ is the image of the function f . Now, by noting that a linear projection map has only eigenvalues 0 and 1, the dimension of $\mathcal{F}(\mathbf{G})$ can be computed by the sum of eigenvalues of $\phi_{\mathbf{G}}$, i.e., $\text{tr}(\phi_{\mathbf{G}})$. Also, using Burnside's lemma, we can count the orbits of \mathbf{G} (acting on $[r]$) by

$$\begin{aligned} |\mathcal{O}(\mathbf{G})| &= \frac{1}{|\mathbf{G}|} \sum_{g \in \mathbf{G}} \text{tr}(P_g) \\ &= \text{tr} \left(\frac{1}{|\mathbf{G}|} \sum_{g \in \mathbf{G}} P_g \right) \\ &= \text{tr}(\phi_{\mathbf{G}}). \end{aligned}$$

Putting together, we get

$$\dim \mathcal{F}(\mathbf{G}) = \text{tr}(\phi_{\mathbf{G}}) = |\mathcal{O}(\mathbf{G})|. \quad (9)$$

Next, we instantiate what we have just shown above for the following case that \mathbf{G} is the following group:

$$\mathbf{G}_0^{\otimes 2} = \{g \otimes g : g \in \mathbf{G}_0\}$$

for some permutation group \mathbf{G}_0 on $[n]$. Note that \mathbf{G} is a permutation group on $[n^2]$. As explained above, $\mathbf{G}_0^{\otimes 2}$ can act on the space of n^2 -dimensional vectors \mathbb{R}^{n^2} . By vectorizing matrices, we can express the space $\mathcal{E}(\mathbf{G}_0)$ of \mathbf{G}_0 -equivariant linear maps on \mathbb{R}^n by

$$\begin{aligned} \text{vec}(\mathcal{E}(\mathbf{G}_0)) &= \{\text{vec}(M) : P_g M P_g^T = M, \forall g \in \mathbf{G}_0\} \\ &= \{\text{vec}(M) : (P_g \otimes P_g) \text{vec}(M) = \text{vec}(M), \forall g \in \mathbf{G}_0\} \\ &= \{\text{vec}(M) : (g \otimes g) \cdot \text{vec}(M) = \text{vec}(M), \forall g \in \mathbf{G}_0\} \\ &= \mathcal{F}(\mathbf{G}_0^{\otimes 2}). \end{aligned}$$

Thus, $|\mathcal{B}(\mathbf{G}_0)| = \dim \text{vec}(\mathcal{E}(\mathbf{G}_0)) = \dim \mathcal{F}(\mathbf{G}_0^{\otimes 2})$. We now calculate the dimension of $\mathcal{F}(\mathbf{G}_0^{\otimes 2})$ using the relationship in (9):

$$\begin{aligned} |\mathcal{B}(\mathbf{G}_0)| &= \dim \mathcal{F}(\mathbf{G}_0^{\otimes 2}) = \text{tr}(\phi_{\mathbf{G}_0^{\otimes 2}}) \\ &= \frac{1}{|\mathbf{G}_0^{\otimes 2}|} \sum_{g \otimes g \in \mathbf{G}_0^{\otimes 2}} \text{tr}(P_{g \otimes g}) = \frac{1}{|\mathbf{G}_0|} \sum_{g \in \mathbf{G}_0} \text{tr}(P_g)^2. \end{aligned} \quad (10)$$

Finally, we complete the proof by calculating the trace formula in (10) for $\mathbf{G}_0 = G \oplus H$, $\mathbf{G}_0 = G \otimes H$, and $\mathbf{G}_0 = H \wr G$:

$$\begin{aligned} |\mathcal{B}(G \oplus H)| &= \frac{1}{|G \oplus H|} \sum_{g \oplus h \in G \oplus H} \text{tr}(P_{g \oplus h})^2 \\ &= \frac{1}{|G||H|} \sum_{g \in G} \sum_{h \in H} (\text{tr}(P_g) + \text{tr}(P_h))^2 \\ &= \frac{1}{|G|} \sum_{g \in G} \text{tr}(P_g)^2 + \frac{1}{|H|} \sum_{h \in H} \text{tr}(P_h)^2 + \frac{2}{|G||H|} \left(\sum_{g \in G} \sum_{h \in H} \text{tr}(P_g) \text{tr}(P_h) \right) \\ &= |\mathcal{B}(G)| + |\mathcal{B}(H)| + 2|\mathcal{O}(G)||\mathcal{O}(H)|, \end{aligned}$$

$$\begin{aligned} |\mathcal{B}(G \otimes H)| &= \frac{1}{|G \otimes H|} \sum_{g \otimes h \in G \otimes H} \text{tr}(P_{g \otimes h})^2 \\ &= \frac{1}{|G||H|} \sum_{g \in G} \sum_{h \in H} \text{tr}(P_g)^2 \text{tr}(P_h)^2 \\ &= |\mathcal{B}(G)||\mathcal{B}(H)|, \end{aligned}$$

$$\begin{aligned} |\mathcal{B}(H \wr G)| &= \frac{1}{|H \wr G|} \sum_{\text{wr}(\vec{h}, g) \in H \wr G} \text{tr}(\text{wr}(\vec{h}, g))^2 \\ &= \frac{1}{|G||H|^p} \sum_{g \in G, (h_1, \dots, h_p) \in H^p} \text{tr} \left(\sum_{i=1}^p \mathbf{1}_{\{i\} \times \{g(i)\}} \otimes P_{h_i} \right)^2 \\ &= \frac{1}{|G||H|^p} \sum_{g \in G, (h_1, \dots, h_p) \in H^p} \left(\sum_{i=1}^p \text{tr}(\mathbf{1}_{\{i\} \times \{g(i)\}} \otimes P_{h_i}) \right)^2 \\ &= \frac{1}{|G||H|^p} \sum_{g \in G, (h_1, \dots, h_p) \in H^p} \left(\sum_{i=1}^p \mathbf{1}_{\{i=g(i)\}} \text{tr}(P_{h_i}) \right)^2 \\ &= \frac{1}{|G||H|^p} \sum_{g \in G, (h_1, \dots, h_p) \in H^p} \left(\sum_{i=1}^p \mathbf{1}_{\{i=g(i)\}} \text{tr}(P_{h_i})^2 + \sum_{i \neq j} \mathbf{1}_{\{i=g(i), j=g(j)\}} \text{tr}(P_{h_i}) \text{tr}(P_{h_j}) \right) \\ &= \frac{1}{|G||H|^p} \sum_{g \in G} \left\{ \sum_{i=1}^p \mathbf{1}_{\{i=g(i)\}} \left(\sum_{(h_1, \dots, h_p) \in H^p} \text{tr}(P_{h_i})^2 \right) \right. \\ &\quad \left. + \sum_{i \neq j} \mathbf{1}_{\{i=g(i), j=g(j)\}} \left(\sum_{(h_1, \dots, h_p) \in H^p} \text{tr}(P_{h_i}) \text{tr}(P_{h_j}) \right) \right\} \\ &= \frac{1}{|G||H|^p} \sum_{g \in G} \left\{ \left(\sum_{i=1}^p \mathbf{1}_{\{i=g(i)\}} \right) |H|^p |\mathcal{B}(H)| + \left(\sum_{i \neq j} \mathbf{1}_{\{i=g(i), j=g(j)\}} \right) |H|^p |\mathcal{O}(H)|^2 \right\} \end{aligned}$$

$$\begin{aligned}
&= \frac{1}{|G|} \sum_{g \in G} \left\{ \left(\sum_{i=1}^p \mathbb{1}_{\{i=g(i)\}} \right) |\mathcal{B}(H)| + \left(\sum_{i=1}^p \mathbb{1}_{\{i=g(i)\}} \sum_{j=1}^p \mathbb{1}_{\{j=g(j)\}} - \sum_{i=1}^p \mathbb{1}_{\{i=g(i)\}} \right) |\mathcal{O}(H)|^2 \right\} \\
&= \frac{1}{|G|} \sum_{g \in G} (\text{tr}(P_g) |\mathcal{B}(H)| + (\text{tr}(P_g)^2 - \text{tr}(P_g)) |\mathcal{O}(H)|^2) \\
&= |\mathcal{O}(G)| |\mathcal{B}(H)| + (|\mathcal{B}(G)| - |\mathcal{O}(G)|) |\mathcal{O}(H)|^2.
\end{aligned}$$

□

Proof of Theorem 2.3 Claims B.1, B.2, and B.3 show that each set of matrices on the right-hand side of the equations in Theorem 2.3 consists of linearly independent matrices, and it is contained in the corresponding space of equivariant linear maps. Furthermore, Claim B.4 shows that the matrices in the set span the whole of the space of equivariant linear maps, since their number coincides with the dimension of the space. Hence, these three claims complete the proof of the theorem.

C Proofs of Theorem 3.1 and Lemma 3.2

Proof of Theorem 3.1 Assume that C is G -equivariant. Pick any $g \in G$. Then, C preserves the standard action of g on \mathbb{R}^n via its permutation matrix. Thus, $Cg = gC$, where g denotes the permutation matrix P_g . This equation is equivalent to

$$g^T C g = C, \quad (11)$$

since $g^T = g^{-1}$. Using this equality, we show that the optimisation objective is invariant with respect to g 's action:

$$\begin{aligned}
\langle C, (Vg^{-1})^T (Vg^{-1}) \rangle &= \langle C, (g^{-1})^T (V^T V) g^{-1} \rangle \\
&= \text{tr}(C^T g (V^T V) g^T) \\
&= \text{tr}((g^T C^T g) (V^T V)) \\
&= \text{tr}((g^T C g)^T (V^T V)) \\
&= \langle g^T C g, V^T V \rangle \\
&= \langle C, V^T V \rangle.
\end{aligned}$$

Here tr is the usual trace operator on matrices, the third equality uses the cyclic property of tr , and the last equality uses (11).

We move on to the proof of the converse. Assume $k = n$ and the equation (3) holds for every $V \in \mathbb{R}^{k \times n}$ and $g \in G$. Pick any $g \in G$. Then, for all $V \in \mathbb{R}^{k \times n}$,

$$\langle C, V^T V \rangle = \langle C, (Vg^{-1})^T (Vg^{-1}) \rangle = \langle g^T C g, V^T V \rangle.$$

The first equality follows from (3), and the second from our derivation above. But the space of matrices of the form $V^T V$ is precisely that of $n \times n$ symmetric positive semi-definite matrices, which is known to contain $n(n+1)/2$ independent elements. Since $n(n+1)/2$ is precisely the dimension of the space of $n \times n$ symmetric matrices, the above equality for every $V \in \mathbb{R}^{k \times n}$ implies that $C = g^T C g$, that is, $Cg = gC$. This gives the G -equivariance of C , as desired.

Proof of Lemma 3.2 Pick arbitrary $V \in \mathbb{R}^{k \times n}$ and $g \in G$. Let v_1, \dots, v_n be the columns of V in order, and v'_1, \dots, v'_n be those of Vg^{-1} in order. Then, $\|v_i\| = 1$ for every $i \in [n]$ if and only if $\|v_{g^{-1}(i)}\| = 1$ for all $i \in [n]$. The latter is equivalent to the statement that $\|v'_i\| = 1$ for every $i \in [n]$.

D Subroutines of SYMFIND

In this section, we describe the subroutines SUMFIND and PRODFIND of our SYMFIND algorithm.

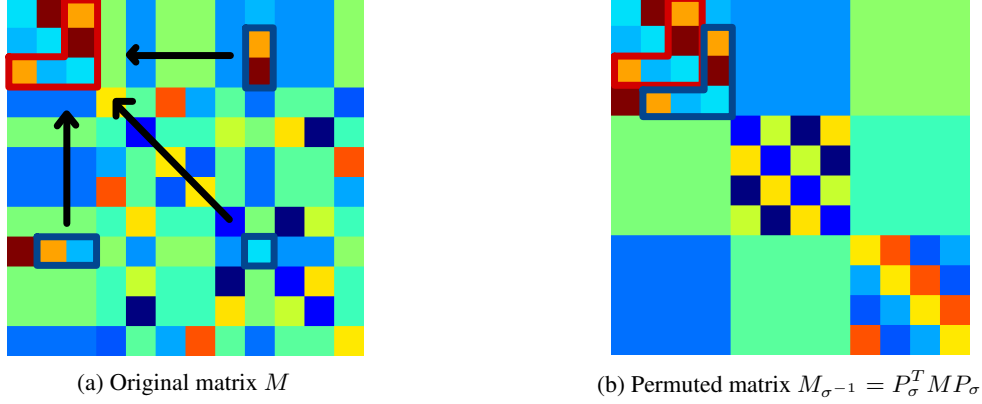


Figure 3: Block pattern which commonly appears in the equivariant matrices under a direct-sum group. In this example, $M_{\sigma^{-1}} \in \mathcal{E}(\mathbb{Z}_4 \oplus \mathbb{Z}_4 \oplus \mathbb{Z}_4)$. The red and blue "L-shaped" clusters have the same values.

D.1 Detection of direct sum

We recall the distributivity law of group constructors [Dummit and Foote, 1991, Majumdar et al., 2012]:

$$\begin{aligned} G \otimes (H \oplus H') &= (G \otimes H) \oplus (G \otimes H'), & (G \oplus G') \otimes H &= (G \otimes H) \oplus (G' \otimes H), \\ G \wr (H \oplus H') &= (G \wr H) \oplus (G \wr H'), & (G \oplus G') \wr H &= (G \wr H) \oplus (G' \wr H). \end{aligned}$$

By this law and the fact that $\mathcal{I}_m = \bigoplus_{i=1}^m \mathbb{Z}_1$ for all m , any permutation group G definable in our grammar can be expressed as a direct sum

$$G = \bigoplus_{i=1}^N H_{(i,1)} \diamond \cdots \diamond H_{(i,n_i)}. \quad (12)$$

where each $H_{(i,j)} \in \{\mathbb{Z}_{m(i,j)}, \mathcal{S}_{m(i,j)}\}$ and \diamond is either \otimes or \wr . Let

$$H_i = H_{(i,1)} \diamond \cdots \diamond H_{(i,n_i)},$$

and p_i be the natural number such that H_i is a permutation group on $[p_i]$. Since both \mathbb{Z}_m and \mathcal{S}_m have only one orbit for all m , each H_i also has only one orbit. Hence, by Theorem 2.3,

$$\mathcal{B}(G) = \bigcup_{i,j \in [N]} B_{ij},$$

where

$$\begin{aligned} B_{ii} &= \{\mathbf{0}_{p_1+\dots+p_{i-1}} \oplus A \oplus \mathbf{0}_{p_{i+1}+\dots+p_N} : A \in \mathcal{B}(H_i)\} \text{ for } i \in [N], \text{ and} \\ B_{ij} &= \{\mathbf{1}_{(p_1+\dots+p_{i-1}+[p_i]) \times (p_1+\dots+p_{j-1}+[p_j])}\} \text{ for } i, j \in [N] \text{ with } i \neq j. \end{aligned}$$

This means that all off-diagonal blocks of any G -equivariant matrices are constant matrices, just like the matrix shown in (b) of Figure 3.

Given a matrix $M \in \mathbb{R}^{m \times m}$, the subroutine SUMFIND aims at finding a permutation $\sigma : [m] \rightarrow [m]$ and the split $m = p_1 + \dots + p_N$ for $p_1, \dots, p_N > 0$ such that $P_{\sigma}^T M P_{\sigma}$ is approximately G -equivariant for some permutation group G on $[m]$ and this group G has the form in (12) where $H_i = H_{(i,1)} \diamond \cdots \diamond H_{(i,n_i)}$ is a permutation group on $[p_i]$. The result of the subroutine is (G, σ) .

SUMFIND achieves its aim using two key observations. The first is an important implication of the G -equivariance condition on $M_{\sigma^{-1}} = P_{\sigma}^T M P_{\sigma}$ that we mentioned above: when the split $m = p_1 + \dots + p_N$ is used to group entries of $M_{\sigma^{-1}}$ into blocks, the G -equivariance of $M_{\sigma^{-1}}$ implies that the off-diagonal blocks of $M_{\sigma^{-1}}$ are constant matrices. This implication suggests one approach: for every permutation σ on $[m]$, construct the matrix $M_{\sigma^{-1}}$, and find a split $m = p_1 + \dots + p_N$ for some N such that off-diagonal blocks of $M_{\sigma^{-1}}$ from this split are constant matrices. Note that this approach is not a feasible option in practice, though, since there are exponentially many permutations σ . The second observation suggests a way to overcome this exponential blow-up issue of the approach. It is that when $M_{\sigma^{-1}}$ is

G -equivariant, in many cases its diagonal blocks are cyclic in the sense that the (i, j) -th entry of a block is the same as the $(i + 1, j + 1)$ -th entry of the block. This pattern can be used to search for a good permutation σ efficiently.

SUMFIND works as follows. It first finds a permutation $\sigma : [m] \rightarrow [m]$ and a split $m = p_1 + \dots + p_N$ using the process that we will explain shortly. Figure 3 illustrates the input matrix M , and its permuted $M_{\sigma^{-1}}$ that has nine blocks induced by the split of $m = p_1 + p_2 + p_3$. Then, SUMFIND calls SYMFIND recursively on each diagonal block of $M_{\sigma^{-1}}$ and gets, for every $i \in [N]$,

$$(H_i, \sigma_i) = \text{SYMFIND}(M_{\sigma^{-1}}[p_{i-1} + 1 : p_i, p_{i-1} + 1 : p_i])$$

where $p_0 = 0$. Finally, SUMFIND returns

$$\left(\bigoplus_{i=1}^N H_i, \sigma \circ \left(\bigoplus_{i=1}^N \sigma_i \right) \right)$$

where

$$\begin{aligned} \sigma_i \oplus \sigma_j &: [p_i + p_j] \rightarrow [p_i + p_j], \\ (\sigma_i \oplus \sigma_j)(a) &= \begin{cases} \sigma_i(a) & \text{if } a \in [p_i], \\ \sigma_j(a - p_i) + p_i & \text{otherwise.} \end{cases} \end{aligned}$$

We now explain the first part of SUMFIND that finds a permutation σ and a split $m = p_1 + \dots + p_N$. For simplicity, we ignore the issue of noise, and present a simpler version that uses equality instead of approximate equality (i.e., being close enough). We start by initialising $\sigma = \sigma_I$, the identity permutation, and $M_{\sigma^{-1}} = M$. Then, we pick an index k_1 from the set $K = \{k_1 \in [2 : m] : (M_{\sigma^{-1}})_{k_1, k_1} = (M_{\sigma^{-1}})_{1,1}\}$. Then, we locate $(M_{\sigma^{-1}})_{1, k_1}$ in the $(1, 2)$ -th entry by swapping the indices 2 and k_1 , which can be done by updating

$$\begin{aligned} M_{\sigma^{-1}} &\leftarrow P_{\sigma(2, k_1)} M_{\sigma^{-1}} P_{\sigma(2, k_1)}^T, \\ \sigma &\leftarrow \sigma \circ \sigma_{(2, k_1)}^{-1}. \end{aligned}$$

Here $\sigma_{(a,b)}(a) = b$, $\sigma_{(a,b)}(b) = a$, and $\sigma_{(a,b)}(c) = c$ for $c \neq a, b$. Next, we find a new index $k_2 \in [3 : m]$ which is suitable to swap with the index 3 in the updated $M_{\sigma^{-1}}$. As Figure 3 shows, we need to find k_2 such that $(M_{\sigma^{-1}})_{2, k_2} = (M_{\sigma^{-1}})_{1,2}$, $(M_{\sigma^{-1}})_{k_2, k_2} = (M_{\sigma^{-1}})_{2,2}$, and $(M_{\sigma^{-1}})_{k_2, 2} = (M_{\sigma^{-1}})_{2,1}$. Once we find such k_2 , we swap the indices 3 and k_2 by updating

$$\begin{aligned} M_{\sigma^{-1}} &\leftarrow P_{\sigma(3, k_2)} M_{\sigma^{-1}} P_{\sigma(3, k_2)}^T, \\ \sigma &\leftarrow \sigma \circ \sigma_{(3, k_2)}^{-1}. \end{aligned}$$

We repeat this process to find an index $k_l \in [l + 1 : m]$ and the "L-shaped" entries which preserve the cyclic pattern. If we cannot find such k_l , we stop the process, and check (i) whether all rows in $(M_{\sigma^{-1}})[1 : l, l + 1 : m]$ are the same and also (ii) whether all columns in $(M_{\sigma^{-1}})[l + 1 : n, 1 : l]$ are the same. If the answers for both (i) and (ii) are yes, we move on to find the next diagonal block in $M_{\sigma^{-1}}$ in the same manner.

If (i) or (ii) has a negative answer, we go back to the step right before choosing k_1 from K and resetting σ and M to the values at that step. Then, we repeat the above process with a new choice of k_1 from K . If no choice of $k_1 \in K$ leads to the situation where both (i) and (ii) have positive answers, then we conclude that $p_1 = 1$, and move on to find the next diagonal block of M starting from the index 2.

D.2 Detection of direct product

Let M be a $m \times m$ matrix. Assume that we are given $p, q \in \mathbb{N}$ with $pq = m$. If for some permutation groups $H \leq \mathcal{S}_p$ and $K \leq \mathcal{S}_q$, the matrix M lies in $\mathcal{E}(H \otimes K)$ (i.e., M is $H \otimes K$ -equivariant), then M can be represented as a linear combination of Kronecker products:

$$M = \sum_{i=1}^{\gamma} (X_i \otimes Y_i) \tag{13}$$

where $X_i \in \mathcal{E}(H)$, $Y_i \in \mathcal{E}(K)$, and γ is a natural number.

The representation suggests the following strategy of finding a group G of symmetries of M that is the direct product of two permutation groups on $[p]$ and $[q]$. First, we express M as a linear combination of Kronecker products $X_i \otimes Y_i$

for $X_i \in \mathbb{R}^{p \times p}$ and $Y_i \in \mathbb{R}^{q \times q}$. Second, we pick a pair X_i and Y_i in the linear combination. Third, we call SYMFIND recursively on X_i and Y_i to get group-permutation pairs (H, σ_H) and (K, σ_K) . Finally, we return $(H \otimes K, \sigma_H \otimes \sigma_K)$ where

$$\begin{aligned} \sigma_H \otimes \sigma_K &: [m] \rightarrow [m], \\ (\sigma_H \otimes \sigma_K)((a-1)q + b) &= (\sigma_H(a) - 1)q + \sigma_K(b) \quad \text{for all } a \in [p] \text{ and } b \in [q]. \end{aligned}$$

Our PRODFIND is the implementation of the strategy just described. The only non-trivial steps of the strategy are the first two, namely, to find the representation of M in (13), and to pick good X_i and Y_i . PRODFIND also has to account for the fact that the representation in (13) holds only approximately at best in our context.

For the representation finding, PRODFIND uses the technique of Van Loan and Pitsianis [1993] that solves the following optimisation problem for given γ :

$$\operatorname{argmin}_{X_i \in \mathbb{R}^{p \times p}, Y_i \in \mathbb{R}^{q \times q}} \left\| M - \sum_{i=1}^{\gamma} (X_i \otimes Y_i) \right\|_F. \quad (14)$$

The technique performs the singular value decomposition of the rearranged matrix $\hat{M} \in \mathbb{R}^{p^2 \times q^2}$ of M defined by

$$\hat{M}_{(i'-1)p+i, (j'-1)q+j} = M_{(i-1)q+j, (i'-1)q+j'} \quad (15)$$

for $i, i' \in [p]$ and $j, j' \in [q]$. To understand why it does so, note that the optimisation problem in (14) is equivalent to the following problem:

$$\operatorname{argmin}_{X_i \in \mathbb{R}^{p \times p}, Y_i \in \mathbb{R}^{q \times q}} \left\| \hat{M} - \sum_{i=1}^{\gamma} \operatorname{vec}(X_i) \operatorname{vec}(Y_i)^T \right\|_F. \quad (16)$$

This new optimisation problem can be solved using SVD. Concretely, if we have the SVD of M , namely,

$$\hat{M} = \sum_{i=1}^{\operatorname{rank}(\hat{M})} s_i (u_i v_i^T) \quad (17)$$

where $\operatorname{rank}(\hat{M})$ is the rank of \hat{M} , s_i is the i -th largest singular value, and u_i and v_i are the corresponding left and right singular vectors, we can solve the minimisation problem (16) by reshaping each term of (17) corresponding to the γ largest singular values, i.e.,

$$\hat{M} \approx \sum_{i=1}^{\gamma} \operatorname{vec}(X_i) \operatorname{vec}(Y_i)^T \quad \text{where } \operatorname{vec}(X_i) = \sqrt{s_i} u_i \text{ and } \operatorname{vec}(Y_i) = \sqrt{s_i} v_i \text{ for every } i \in [\gamma].$$

The first step of PRODFIND is to apply the technique of Van Loan and Pitsianis [1993]. PRODFIND performs the SVD of the matrix \hat{M} and gets s_i, u_i, v_i in (17) where $s_1 \geq s_2 \geq \dots \geq s_l$ for some l . Then, it sets $L = s_1/5$, and picks γ so that all i 's with $s_i \geq L$ are included when we approximate \hat{M} .

The second step of PRODFIND is to pick X_i and Y_i . PRODFIND simply picks X_1 and Y_1 that correspond to matrices (reshaped from u_1 and v_1) for the largest singular value s_1 . We empirically observed that the matrices X_1 and Y_1 are most informative about the symmetries of M , and are least polluted by noise from the training of SATNet.

The third and fourth steps of PRODFIND are precisely the last two steps of the strategy that we described above.

Our description of SYMFIND in the main text says that PRODFIND gets called for all the divisors p of n with q being n/p , since we do not know the best divisor p a priori, and that each invocation generates a new candidate in the candidate list \mathcal{A} . However, in practice, we ignore some divisors that violates our predefined criteria. In particular, we set an upper bound U on γ , and use a divisor p only when PRODFIND for p picks γ with $\gamma \leq U$, i.e., not too many terms are considered in the linear combination of Kronecker products. This criterion can be justified by the following lemma:

Lemma D.1. *Let $G = H \otimes K$ be the direct product of permutation groups H and K on $[p]$ and $[q]$, respectively. Consider a G -equivariant matrix $M \in \mathcal{E}(G)$ and its rearranged version \hat{M} in (15). Then, $\operatorname{rank}(\hat{M}) \leq \min(|\mathcal{B}(H)|, |\mathcal{B}(K)|)$.*

Proof. Let $M \in \mathcal{E}(G)$. The matrix M can be expressed as a linear combination of the basis elements in $\mathcal{B}(G)$:

$$\begin{aligned} M &= \sum_{i=1}^{|\mathcal{B}(H)|} \sum_{j=1}^{|\mathcal{B}(K)|} \alpha_{ij} (A_i \otimes B_j) \\ &= \sum_{j=1}^{|\mathcal{B}(K)|} \left(\sum_{i=1}^{|\mathcal{B}(H)|} \alpha_{ij} A_i \right) \otimes B_j \end{aligned} \tag{18}$$

$$= \sum_{i=1}^{|\mathcal{B}(H)|} A_i \otimes \left(\sum_{j=1}^{|\mathcal{B}(K)|} \alpha_{ij} B_j \right) \tag{19}$$

where $A_i \in \mathcal{B}(H)$ and $B_j \in \mathcal{B}(K)$. We can also rewrite (18) and (19) with equations for \hat{M} :

$$\hat{M} = \sum_{j=1}^{|\mathcal{B}(K)|} \text{vec}(A'_j) \text{vec}(B_j)^T = \sum_{i=1}^{|\mathcal{B}(H)|} \text{vec}(A_i) \text{vec}(B'_i)^T$$

$$\text{where } A'_j = \left(\sum_{i=1}^{|\mathcal{B}(H)|} \alpha_{ij} A_i \right) \text{ and } B'_i = \left(\sum_{j=1}^{|\mathcal{B}(K)|} \alpha_{ij} B_j \right).$$

Since the summands $\text{vec}(A'_j) \text{vec}(B_j)^T$ and $\text{vec}(A_i) \text{vec}(B'_i)^T$ are rank-1 matrices, by the subadditivity of rank, i.e., $\text{rank}(X + Y) \leq \text{rank}(X) + \text{rank}(Y)$, we have $\text{rank}(\hat{M}) \leq \min(|\mathcal{B}(H)|, |\mathcal{B}(K)|)$. \square

Having fewer basis elements is generally better because it leads to a small number of parameters to learn in SymSATNet. The above lemma says that a divisor p with large γ (which roughly corresponds to the large rank of \hat{M} in the lemma) leads to large $|\mathcal{B}(H)|$ and $|\mathcal{B}(K)|$. Our criterion is designed to avoid such undesirable cases.

D.3 Detection of wreath product

Assume that the permutation groups G and H act transitively on $[p]$ and $[q]$ (i.e., for all $i, j \in [p]$ and $i', j' \in [q]$, there are $g \in G$ and $h \in H$ such that $g(i) = j$ and $h(i') = j'$). We recall that in this case, every equivariant matrix M under the wreath product of groups $H \wr G$ can be expressed as follows [Wang et al., 2020]:

$$M = A \otimes \mathbf{1}_q + I_p \otimes B \tag{20}$$

for some $A \in \mathcal{E}(G)$ and $B \in \mathcal{E}(H)$, where $\mathbf{1}_m, I_m$ are everywhere-one, identity matrices in $\mathbb{R}^{m \times m}$. We use this general form of $\mathcal{B}(H \wr G)$ -equivariant matrices and make PRODFIND detect the case that symmetries are captured by a wreath product.

Our change in PRODFIND is based on a simple observation that the form in (20) is exactly the one in (13) with $\gamma = 2$. We change PRODFIND such that if we get $\gamma = 2$ while running $\text{PRODFIND}(M, p)$, we check whether M can be written as the form in (20). This checking is as follows. Using given p and q , we create blocks

$$M^{(i,j)} = M[(i-1) \times q + 1 : i \times q, (j-1) \times q + 1 : j \times q]$$

of $q \times q$ submatrices in M for all $i, j \in [p]$. Then, we test whether all $M^{(i,i)} - M^{(j,j)}$ and $M^{(i,j)}$ for $i \neq j$ are constant matrices (i.e., matrices of the form $\alpha \mathbf{1}_q$ for some $\alpha \in \mathbb{R}$). If this test passes, M has the desired form. In that case, we compute A and B from M , and recursively call SYMFIND on A and B .

We can also make SUMFIND(M) detect wreath product. The required change is to perform a similar test on each diagonal block of the final $M_{\sigma-1}$ computed by SUMFIND(M). The only difference is that when the test fails, we look for a rearrangement of the rows and columns of the diagonal block that makes the test succeed. If the test on a diagonal block succeeds (after an appropriate rearrangement), the group corresponding to this block, which is one summand of a direct sum, becomes a wreath product.

E Symmetries in Sudoku and Rubik’s Cube Problems

In this section, we describe the group symmetries in Sudoku and the completion problem of Rubik’s cube. In both problems, we can find certain group $G \leq \mathcal{S}_n$ acting on $\mathbb{R}^{k \times n}$ such that for any valid assignment $V \in \mathbb{R}^{k \times n}$ of problem, $g \cdot V$ is also valid for any $g \in G$.

In 9×9 Sudoku, we denote the first three rows of a Sudoku board by the first band, and the next three rows by the second band, and the last three rows by the third band. In the same manner, we denote each three columns by a stack. For Sudoku problem, one can observe that any row permutations within each band preserve the validity of the solutions. Also, the permutations of bands preserve the validity. We can represent this type of hierarchical actions by wreath product groups. In this case, 3 bands are permuted in a higher level, and 3 rows in each band are permuted in a lower level, which corresponds to the group action of $\mathcal{S}_3 \wr \mathcal{S}_3$. The same process can be applied to the stacks and the columns, which also corresponds to the group $\mathcal{S}_3 \wr \mathcal{S}_3$. Furthermore, the permutations of number occurrences in Sudoku (e.g., switching all the occurrences of 3’s and 9’s) also preserves the validity of the solutions. In this case, any permutations over [9] are allowed, thus \mathcal{S}_9 represents this permutation action. Overall, we have three permutation groups, $G_1 = \mathcal{S}_3 \wr \mathcal{S}_3$, $G_2 = \mathcal{S}_3 \wr \mathcal{S}_3$, and $G_3 = \mathcal{S}_9$. These three groups are in different levels; G_1 is at the outermost level, and G_3 is at the innermost level. Note that these three types of actions are commutative, i.e., the order does not matter if we apply the actions in different levels. This relation forms a direct product between each level, and we conclude $G = (\mathcal{S}_3 \wr \mathcal{S}_3) \otimes (\mathcal{S}_3 \wr \mathcal{S}_3) \otimes \mathcal{S}_9$.

For Rubik’s cube, we first introduce some of the conventional notations. We are given a $3 \times 3 \times 3$ Rubik’s cube composed of 6 faces and 9 facelets in each face. There are also 26 cubies in the Rubik’s cube, and they are classified into 8 corners, 12 edges, and 6 centers. To change the color state of Rubik’s cube, we can move the cubies with 9 types of rotations, which are denoted by $U, D, F, B, L, R, M, E, S$. We can represent each color state of the Rubik’s cube by a function from $F = [6] \times [9]$ to $C = [6]$, where F encodes the face and facelets, and C encodes the colors. The initial state of Rubik’s cube is $s : F \rightarrow C$ satisfying $s(i, j) = i$ for all $(i, j) \in F$. If there exists a sequence of rotations that transforms s to the initial state, then s is solvable. Our completion problem of Rubik’s cube is to find a color assignment such that the assignment is solvable. For example, if a corner cubie contains 2 same colors, it is not solvable because these adjacent same colors cannot be separated by the 9 types of rotations.

We can observe the following group symmetries in the completion problem of Rubik’s cube: any solvable color state is still solvable after being transformed by the 9 types of rotations. These 9 rotations generate a permutation group \mathcal{R}_{54} acting on the 6×9 facelets of a Rubik’s cube, which is called the Rubik’s cube group. Furthermore, like Sudoku, we can also consider the permutations of color occurrences. In this case, if we assume the colors 0 and 5 are initially on the opposite sides, then the solvability can be broken by switching the colors 0 and 1 since the colors 0 and 5 are then no longer on the opposite sides. Considering this, computing all possible permutations acting on the color occurrences is not trivial. Instead, we can generate such group \mathcal{R}_6 by 3 elements, each of which corresponds to the 90° rotation in one of the three axes in 3-dimension. Finally, these two groups \mathcal{R}_{54} and \mathcal{R}_6 form different levels of actions, and actions from different levels commute each other. Therefore, we conclude $G = \mathcal{R}_{54} \otimes \mathcal{R}_6$.

F Forward-pass and Backward-pass Algorithms of SymSATNet

Our SymSATNet includes forward-pass and backward-pass algorithms as described in Section 3. Here, we describe slight changes of the forward-pass and backward-pass algorithms in SymSATNet, and the improvement of efficiency obtained by these changes. In Algorithm 2 and Algorithm 3, we let c_o be the o -th column of the matrix C , and v_o^{prev} and u_o^{prev} be the previous o -th columns of V and U before the update. Also, let $P_o = I_k - v_o v_o^T$, and $\mathbb{1}_o$ be the n -dimensional one-hot vector whose only o -th element is 1. Note that our algorithm is only slightly different from the one of original SATNet, and the only difference is that the inner products $s_i^T s_j$ are substituted by $C_{i,j}$ which can be directly derived from $C = S^T S$. This allows us to implement the forward-pass and the backward-pass algorithm of SymSATNet in the same manner as the original SATNet.

The above changes bring the speed up in matrix operations. In SymSATNet, we can skip a matrix multiplication $V S^T$ where $V \in \mathbb{R}^{k \times n}$ and $S \in \mathbb{R}^{m \times n}$, which was required in the original SATNet for the rank-1 update. Also, we can simply use $C_{i,j}$ without calculating $s_i^T s_j$. Finally, the rank-1 updates of the original SATNet are revised by a column update: $V = V + (v_o - v_o^{\text{prev}}) \mathbb{1}_o^T$ and $U = U + (u_o - u_o^{\text{prev}}) \mathbb{1}_o^T$. As a consequence, these substitutions improve the speed of the training process of SymSATNet.

Algorithm 2 Forward pass of SymSATNet

Input: $V_{\mathcal{I}}$
init random unit vectors $v_o, \forall o \in \mathcal{O}$
repeat
 for $o \in \mathcal{O}$ **do**
 compute $g_o = Vc_o - C_{o,o}v_o$
 compute $v_o = -g_o / \|g_o\|$
 update $V = V + (v_o - v_o^{\text{prev}})\mathbb{1}_o^T$
 end for
until not converged
Output: $V_{\mathcal{O}}$

Algorithm 3 Backward pass of SymSATNet

Input: $\{\partial\ell/\partial v_o : o \in \mathcal{O}\}$
init $U_{\mathcal{O}} = 0$
repeat
 for $o \in \mathcal{O}$ **do**
 compute $dg_o = Uc_o - C_{o,o}u_o - \partial\ell/\partial v_o$
 compute $u_o = -P_o dg_o / \|g_o\|$
 update $U = U + (u_o - u_o^{\text{prev}})\mathbb{1}_o^T$
 end for
until not converged
Output: $U_{\mathcal{O}}$

G Hyperparameters

In this section, we specify the hyperparameters to run SymFind algorithm and the validation steps in SymSATNet-Auto. Each validation step requires a threshold of improvement of validation accuracy to measure the usefulness of each smaller part in a given group. We set this threshold by 0.05 for all validation steps, i.e., only the smaller parts showing improvement greater than 0.05 were considered to be useful, and were combined to construct the whole group. Also, our SymFind algorithm receives λ as an input, which determines the degree of sensitivity of SymFind. In practice, this tolerance was implemented by two hyperparameters, say λ_1 and λ_2 . λ_1 was used to compute a threshold to decide whether a pair of entries have the same value within our tolerance so that they have to be clustered. We computed this threshold by the multiplication of λ_1 and the norm of input matrix, and λ_1 was fixed by 0.05 in Sudoku, and 0.1 in Rubik’s cube. λ_2 played a role of a threshold to conclude that the input matrix truly has the symmetries under the discovered group by SymFind. λ_2 was used in the last step of SymFind, where the largest group is selected among the candidates. With the Reynolds operator, we computed the distance between the input matrix and the equivariant space under each candidate group, and filtered out the groups whose distance is greater than λ_2 . We determined λ_2 by the number of corruption in the dataset; 0.4 for the dataset with 0 corruption, 0.5 for 1 corruption, 0.55 for 2 corruption, and 0.6 for 3 corruption.

H GPU Usage

The implementation of SymSATNet is based on the original SATNet code, and thus the calculations in the forward-pass and the backward-pass algorithms of SymSATNet can be accelerated by GPU. We used GeForce RTX 2080 Ti for every running of SATNet and SymSATNet.